

National Aeronautics and Space Administration



Reliability of Recolunmed Area Array Packages

Reza Ghaffarian, Ph.D.
Jet Propulsion Laboratory
Pasadena, California

Jet Propulsion Laboratory
California Institute of Technology
Pasadena, California

JPL Publication 09-11 3/09



Reliability of Recolumned Area Array Packages

NASA Electronic Parts and Packaging (NEPP) Program
Office of Safety and Mission Assurance

Reza Ghaffarian, Ph.D.
Jet Propulsion Laboratory
Pasadena, California

NASA WBS: 939904.01.11
JPL Project Number: 103982
Task Number: 03.03.07

Jet Propulsion Laboratory
4800 Oak Grove Drive
Pasadena, CA 91109

<http://nepp.nasa.gov>

This research was carried out at the Jet Propulsion Laboratory, California Institute of Technology, and was sponsored by the National Aeronautics and Space Administration Electronic Parts and Packaging (NEPP) Program.

Reference herein to any specific commercial product, process, or service by trade name, trademark, manufacturer, or otherwise, does not constitute or imply its endorsement by the United States Government or the Jet Propulsion Laboratory, California Institute of Technology.

Copyright 2009. California Institute of Technology. Government sponsorship acknowledged.

Objectives and Products

Commercial, off-the-shelf area array packaging (COTS AAP) technologies in high reliability versions are now being considered for use in a number of NASA electronics systems. Understanding the process and QA indicators for reliability as well as rework challenges are important for the low risk insertion of these newly available packages. The objectives of this task are to develop qualification guidelines based on assembly reliability test data for reworked, recolumned, and reassembled ceramic column grid array (CCGA) packages. CCGA columns are fragile and may be bent or damaged during shipping and handling and/or form defective joints during assembly. It may be decided to recolumn an existing package rather than replace the package. Delays in schedule and/or the high cost of replacement play significant roles in the final decision. The option of recolumning requires careful evaluation of subsequent assembly risk since package/die is considered prequalified for its original assembly.

This report first presents a literature survey for CCGA electronics package technologies with emphasis on assembly reliability. Then, it presents rework and recolumning of two high input/output (I/O) CCGA packages: one with a full column population and the other with a peripheral column configuration. Subsequent to recolumning and after one additional reflow, packages were subjected to isothermal aging to determine the integrity of columns and tin-lead solder attachments. As-built integrity and degradation with time were determined by a tensile testing method specifically developed for this purpose and are presented in this report. Individual tensile strength test data and their plots showing strength reduction with time due to a high temperature aging are also presented.

In addition, the process control parameters for assembly of recolumned packages using either vapor phase or rework stations were established for both package types. Details of these process control parameters as well as quality assurance indicators based on visual inspection before and during thermal cycling tests are presented. Qualification guidelines generated based on these and additional optical photomicrographs, X-rays, SEMs, and destructive cross-sectioning of thermally cycled, reworked, recolumned, and reassembled test vehicles of the two high I/O packages are presented in detail. The qualification guidelines based on test results will facilitate NASA projects use of high I/O CCGA packages, with more processing power in a smaller board footprint, both for virgin and reworked assemblies.

Table of Contents

1. Organization and Topics of Report	1
2. Executive Summary	3
3. Background Information	7
3.1 Introduction.....	7
3.2 Survey: CCGA Reliability	9
3.3 Effect of Solder Joint Volume on CCGA Assembly Reliability	10
3.4 Failure Mechanisms of CCGA 560 I/Os.....	11
3.5 NASA and Industry Standards for Assembly, Rework, and Thermal Cycle.....	12
3.6 Attachment Procedures	12
3.7 X-ray Characterizations	13
3.8 Scanning Electron Microscopy Characterizations.....	13
3.9 Thermal Cycle Profiles	14
4. Experimental Approaches—Recolumn of CCGA 560 I/Os	15
4.1 Purpose for Using CCGA 560 I/Os	15
4.2 Key Rework, Recolumn, and Reassembly Parameters for 560 I/Os	16
4.3 Pull Strength Cu Spiral Columns Attachment Pre- and Post-Aging	18
4.4 PWB/TV/Package CCGA 560 I/Os	23
4.5 Recolumn and Reassembly of CCGA 560 I/Os.....	24
4.6 Inspection after Reassembly	25
4.7 Test Results for Recolumned/Reassembled CCGA560 I/Os.....	27
4.7.1 <i>Thermal Cycle Conditions</i>	27
4.7.2 <i>X-ray Characterization</i>	27
4.7.3 <i>Optical Photomicrographs of Damage Progress with Thermal Cycles</i>	28
4.7.4 <i>SEM Photomicrographs and X-section</i>	31
5. Experimental Approaches for High I/O CCGA	36
5.1 Evaluation of High I/O CCGA	36
5.2 PWB/Package Recolumn	37
5.3 Stencil Design, Paste Deposition, and Volume Measurement.....	39
5.4 Inspection before Environmental Tests	42
5.5 Test Results after Thermal Cycling for High I/O Assemblies.....	46
5.5.1 <i>Thermal Cycle Condition</i>	46
5.5.2 <i>Damage Progress Characterizations by Optical Microscopy</i>	46
5.5.3 <i>SEM Photomicrographs and X-section</i>	46
5.6 Failure Behavior of a High I/O CBGA.....	49
6. Conclusions	51
7. NASA Applications	53
8. Acronyms and Abbreviations	54

9. Acknowledgements 56
10. References 57
11. Vendor Report on Column Attachment Strengths 59

1. Organization and Topics of Report

This report first provides a body of knowledge (BoK) literature survey for low-to-high I/O ceramic column grid array (CCGA) packages that have potential for use in NASA electronic systems. It then presents process data on rework, recolumn attachment, tensile test data after isothermal aging, and thermal cycle testing after reassembly of recolumned packages onto printed wiring boards (PWBs). Furthermore, it includes optical and scanning electron microscopy (SEM) photographs from various tests at intervals, showing rework process quality and damage progress with cycling. In addition, failure analyses from non-destructive evaluation by X-ray and destructive characterization by X-sectioning are presented. Finally, it summarizes lessons learned based on reliability test results and provides recommendations for NASA use. Topics discussed in this report are as follows:

- Executive summary providing key background information, test results, and lessons learned for virgin, rework, and recolumned packages and reassembled test vehicles before and after thermal cycling.
- Summary of key parameters that affect assembly reliability of CCGAs.
- Comparison of the effects of solder volumes on assembly reliability for CCGAs and ceramic ball grid arrays (CBGAs).
- Brief discussion on failure mechanisms for the virgin CCGA 560 I/O (1.27-mm pitch) assemblies subjected to thermal cycling in a previous investigation.
- Documentation covering recolumning of CCGA 560 I/Os using a smaller column diameter that is attached directly to the package, replacing the original package with a larger column and an interposer layer between the column and package.
- Tensile test results for recolumned 560 I/O packages before and after isothermal aging at 125°C for 500 hours. One package had an additional reflow representing one more assembly reflow condition.
- Quality assurance documentation of reassembly processes using either vapor phase or rework stations for the 560 I/O recolumned packages. Packages were assembled onto printed wiring boards (PWBs) with pads designed for ceramic or plastic packages (PBGA 560 I/Os) using two different ministencils, representing real rework paste print condition. Included photomicrographs of paste print quality and their estimated volumes based on area and height values determined by profilometer.
- Photomicrographs of representative solder paste deposition exhibiting quality and estimated solder volume by laser measurement for a high I/O CCGA, 1 mm pitch and two column sizes, where two ministencils with two thicknesses and two apertures sizes were used to optimize solder volume.
- Optical photographs of representative assemblies with and without manufacturing workmanship defects for as-built recolumned CCGA 560 I/O packages.

- Thermal cycle reliability test results for recolumned CCGA 560 I/O assemblies considered to have acceptable solder joint quality condition after visual inspection and daisy chain verification.
- Documentation and photomicrographs for full array, recolumned, high I/O CCGA packages with 1-mm pitch and 22- and 15-mils diameter columns.
- Optical photomicrographs for reassembly of recolumned, high I/O CCGA packages onto PWBs using two different ministencil thicknesses and aperture sizes (reassembled using either a reflow vapor phase machine or rework station).
- Optical photomicrographs of recolumned, high I/O CCGA assemblies during thermal cycling performed at intervals to document damage progress for various processes and thermal cycle conditions.
- Thermal cycle reliability test results for up to 1000 cycles in the range of $-55^{\circ}/+100^{\circ}\text{C}$, $-55^{\circ}/+125^{\circ}\text{C}$, and $-120^{\circ}/+85^{\circ}\text{C}$ for selective recolumned CCGA assemblies.
- X-ray photomicrographs and characterization of assemblies performed to determine quality assurance indicators and to establish if a 2D X-ray technique can be used to detect damage, including cracks, due to thermal cycling.
- Scanning electron microscopy (SEM) and energy dispersive X-ray (EDX) mapping photomicrographs of thermally cycled CCGA assemblies. These were performed only after the test vehicles were cut into samples in preparation for cross-sectioning evaluation.
- Photomicrographs of X-sectioned, thermally cycled CCGA assemblies documenting damage progress and failures in order to correlate destructive and non-destructive observations.
- Failure mechanisms for assemblies with high I/O CBGA packages that were subjected to thermal cycling at JPL but built by an electronics manufacturing service (EMS) company as a collaborative effort.
- In section 6—Conclusion, a summary of the key findings for virgin and recolumned CCGA assemblies.
- In section 7—NASA Applications, specific overall recommendations for NASA and industry to facilitate CCGA technology insertion for high reliability electronic systems.

2. Executive Summary

This report presents qualification guidelines developed for recolumned, high I/O ceramic column grid array (CCGA) packages assembled onto printed wiring/circuit boards (PWBs/PCBs). It includes recolumn and assembly process development for two types of CCGA packages: those with and those without interposer. Figure 1 compares the CCGA package with interposer (a thin layer of ceramic between package and column) with its recolumned package where the interposer was removed prior to recolumning. Thermal cycle test results and photomicrographs showing damage progress for recolumned CCGA assemblies are documented and presented.

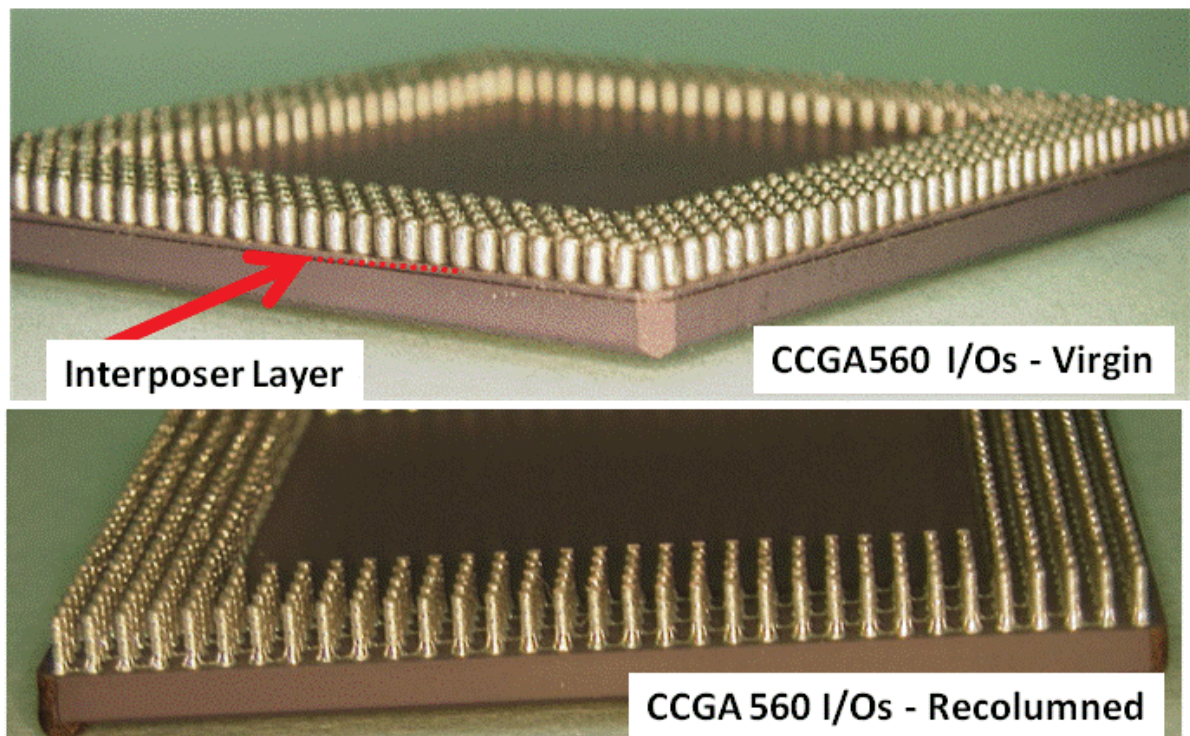


Figure 1. Virgin CCGA 560 I/O package with interposer (top) and recolumned package with no interposer (bottom).

For high reliability applications, surface mount leaded packages, such as ceramic quad flat packs (CQFPs), are now being replaced with CCGAs with a 1.27-mm pitch (distance between adjacent ball centers) or lower. Replacement is especially appropriate for packages with higher than 300 I/O counts where CQFP pitches become fine, making them extremely difficult to handle and assemble. In addition to size reduction, CCGAs also provide improved electrical and thermal performance; however, their solder columns are prone to damage, and it is almost impossible to rework defective solder joints. Rework, recolumn, and reassembly may be required to address solder defects due to processing or column damage prior to assembly due to shipping and mishandling. Package recolumn integrity as well assembly reliability is addressed herein.

CCGA packages are preferred to CBGA (see Figure 2) since they show better thermal solder joint reliability than their CBGA counterparts. Superior reliability is achieved for larger packages and for higher than 300 I/Os when resistance to thermal cycling is further reduced with increasing package size. All ceramic packages with more than about 1,000 I/Os come in the CCGA style with 1-mm pitch or lower in order to limit growth of the package size.

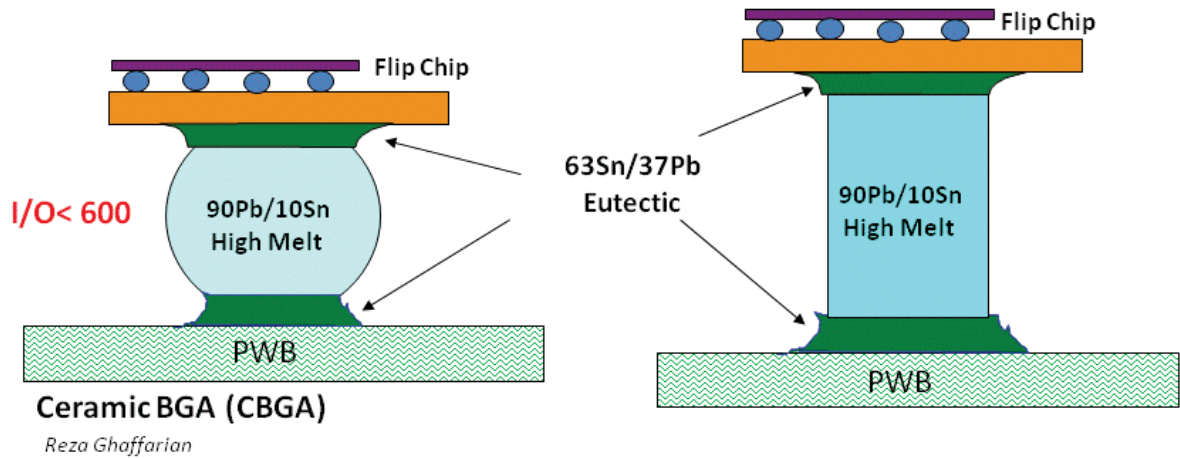


Figure 2. Examples of ceramic column grid array (CCGA) and ceramic ball grid array (CBGA) package configurations.

In summary, key recent trends in electronic packages for high reliability applications are as follows:

- Ceramic quad flat pack (CQFP) to area array packages
- CBGA to CCGA/CGA (>500 I/Os) and land grid array (LGA)
- Wire-bond to flip-chip die within a package
- Hermetic to non-hermetic packages (>1000 I/Os)
- High-lead solder columns to columns with Cu wrap
- Pb-Sn to Pb-free, including potential use of a Cu column
- Land grid with conductive interconnects rather than Pb-free solder

The key drawback of CCGAs remains the same: individual column re-workability and inspection capability for interconnection integrity is poor (e.g., cracks and cold solder). Implementation of process controls is critical to achieving quality solder joints, which consequently achieves optimum assembly reliability. Visual inspection of peripheral columns, when they are not blocked, can be performed by optical microscopy to ensure solder quality as another process indicator. Although progress has been made in improving the resolution of X-ray for better inspection, the issue of inspection remains partially unresolved.

Even though CCGAs are commercial, off-the-shelf (COTS) packages, their high reliability package versions go through a more stringent screening with added cost and long-time delay in delivery schedule. The issues with CCGA COTS packages are essentially the same as other COTS issues and include package die source and materials variations from lot to lot, availability of packages with radiation-hard die, outgassing for materials, etc. Assembly, inspection, and lack of individual solder reworkability issues are additional key aspects of such implementation. Assembly reliability behaviors of such packages are addressed in previous investigations [1]–[3].

To address requirements for reworking of columns either due to package mishandling or assembly workmanship defects, columns of the package are required to be removed and new columns attached. Rework and recolumn solder attachments were evaluated using two CCGA packages, each with unique features.

One package with 560 columns in a five-row periphery, 1.27-mm pitch, and 42.5-mm size had an additional interposer added by the manufacturer to decrease thermal coefficient of thermal expansion (CTE) mismatch. Several of the virgin packages were recolumned after removal of the interposer and then reassembled onto the board. In addition, a few of the packages were assembled onto the board first before reworking and recolumning but after interposer removal. Subsequently, acceptable reassemblies were subjected to environmental evaluation and failure analyses.

The second CCGA package had more than 1,000 columns, was fully populated, and had a lower pitch of 1 mm and package body size of 35 mm. Assemblies were reworked and recolumned using 22- and 15-mm diameter columns and reassembled using a vapor phase machine and a rework station. Figure 3 depicts representative photomicrographs of a high I/O CCGA package after recolumning before reassembly. Note quality of solder joints at a higher magnification exhibiting excellent quality with smooth and shiny appearance and good fillet formation.

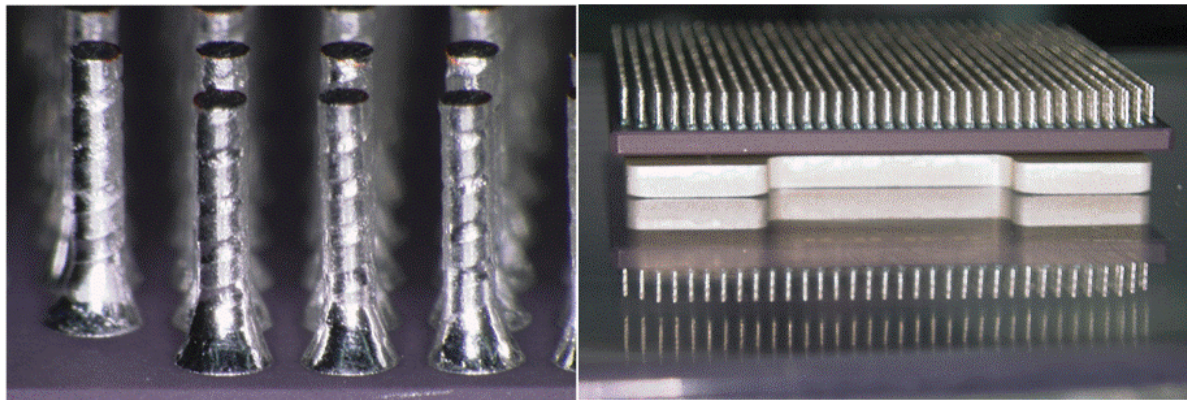


Figure 3. Representative of a recolumned, high I/O CCGA package with a photomicrograph showing corner columns at a higher magnification.

Several recolumned packages were subjected to pull testing prior to and after high temperature storage to determine the strength of the Cu spiral column and attachment and to establish strength degradation with time. The as-recolumned samples showed ductile failures in column with no failures at the attachment interconnections. The average force

was 1340 g with a standard deviation of 137 g, a very consistent column quality with no interfacial failure. Pull strengths were also evaluated after an additional reflow and exposure to 125°C for up to 500 hours. The average pull-strength values decreased rapidly initially and then slowed down with time, for a total decrease of 19% at 500 hours.

For a relatively larger 560 I/O package, many challenges were encountered during recolumning and reassembling. Based on successful reassembly test vehicles, it was shown that for the 560 I/O package, the interposer interconnections are sources for failure during thermal cycling; therefore, removing this source of weakness may potentially improve reliability if the original column size is used. This postulate was not verified since a smaller column size was used in this investigation. The second package assembly exhibited visually acceptable solder joint quality with no early failures during thermal cycling. Representative optical photomicrographs for the package assemblies showing damage progress during thermal cycling are also presented. SEM was performed on a thermally cycled failed package prior to and after X-sectioning. Signs of microcracks at the package solder interface surrounding the package pads were apparent. It was confirmed through X-sectioning that a number of these microcracks were fully penetrated through solder interconnection at the package side. The results are consistent with daisy chain opening for the package detected prior to optical and SEM characterizations.

Twelve high I/O CCGA packages were successfully recolumned and reassembled using rework station for package placement and using either a vapor phase or a rework station for solder paste reflowing. Representative optical photomicrographs showing damage progress due to thermal cycling for both column sizes are presented in this report. Assemblies passed 200 severe thermal cycles with no apparent visual damage or daisy chain failures. However, damage and fine microcracks were apparent at higher cycles. Representative optical and SEM photomicrographs at higher magnifications with microstructural resolution showing microcracks at the package side are also presented. Signs of microcracks were also apparent in the column at the Cu spiral interface.

To achieve the confidence level necessary for specific application, larger samples should be used to further validate these preliminary test results. Note also that the effects of three or more reflow exposures due to rework/recolumn/reassembly on active die functionality are unknown since packages evaluated in this investigation had dummy daisy chain die rather than functional die. Even though most package suppliers perform a limited number of reflow exposures as a part of their qualification flow, this is an aspect of this technology that should be considered before acceptance of recolumn/reassembly for a critical application.

3. Background Information

3.1 Introduction

Examples of typical area array packages are shown in Figure 4. These include plastic ball grid arrays with ball eutectic compositions of Sn₆₃/Pb₃₇ alloy or a slight variation. The CBGA package uses a higher melting ball (Pb₉₀/Sn₁₀) with eutectic solder attachment to the die and board. Column grid array (CGA or CCGA) is similar to BGA except it uses column interconnects instead of balls. Flip-chip BGA (FCBGA) is similar to BGA, except it is internal to the package and flip-chip die are used.

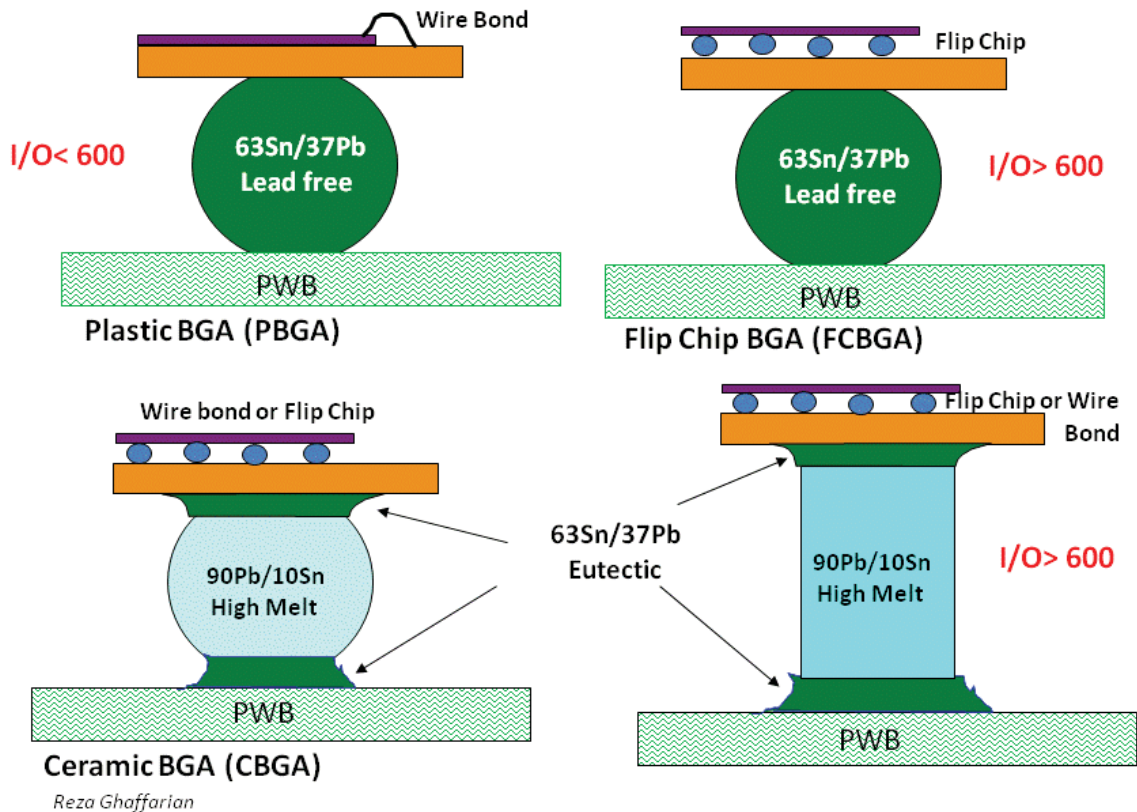


Figure 4. Representative key area array package (AAP) configurations: BGA, FCBGA, CBGA, and CCGA.

CCGAs offer several distinct advantages over fine pitch surface mount components having gull wing leads, including:

- High I/O capability. Hundreds up to 2,000 balls/columns can be built and manufactured, but gull-wing leads are limited to less than 300 I/Os.
- Larger column pitches for the same I/Os, which significantly reduce the manufacturing complexities for high I/O parts.

- Higher packaging densities are achievable since, for CCGAs, area rather than periphery of the package is utilized and no additional package periphery is needed to accommodate leads extension; therefore, it is possible to mount more packages per board, i.e., higher packaging density.
- Faster circuitry speeds than gull-wing surface mount components (SMCs) because the terminations are much shorter and, therefore, less inductive and resistive.
- Better heat dissipation.
- Conventional surface mount technology (SMT) such as stencil printing and component mounting can be employed.

However, the key disadvantages of CCGA include its lack of compatibility with multiple solder processing methods and lack of individual solder joint inspectability and reworkability using conventional methods. For high reliability applications, the ability to inspect the solder joints visually has been a standard inspection requirement and is a key factor for providing confidence in the solder joint reliability. Advanced inspection tools, including X-rays, need further development to provide such confidence for CCGAs.

The five chief drawbacks of CCGAs are as follows:

- Lack of direct visual inspection capability.
- Need for a multilayer PWB because of dense interconnect routing between the chip and the PWB.
- Reduction in resistance to thermal cycling due to use of rigid columns.
- Lack of individual solder joint reworkability.
- Requirement for recolumning to meet a tight schedule and/or reduce cost if columns or solder joints are damaged during either the handling or the assembly process.

NASA and the NASA-led Consortia have performed extensive research [1]–[9] in order to understand the technology implementation of area array packages for high reliability applications. The work included the study of process optimization and assembly reliability characterization as well as the use of inspection tools, including X-ray and optical microscopy, for quality control and damage detection due to environmental exposures. Recent activities also covered CCGA package assembly reliability, including the effects of corner staking and conformal coating.

The ceramic BGA package uses a higher melting ball ($\text{Pb}_{90}\text{Sn}_{10}$) with eutectic attachment to the die and board. The column grid array (CGA) or ceramic column grid array (CCGA) is similar to a CBGA except that it uses column interconnects instead of balls. The lead-free CCGA uses a Cu instead of a high-melting, lead/tin column. The flip-chip BGA (FCBGA) is similar to the BGA, except that, internally, a flip-chip die rather than a wire bonded die is used.

Three array configurations are popular: full array, peripheral array, and staggered array with single pitch. Recently, area arrays with mixed pitches have also been developed for specific applications, making design and processing more complex. Plastic array packages come in all styles, whereas ceramic package are generally limited to a full array

configuration. Especially for high I/O and low pitch packages, fully populated array packages present some significant routing challenges if a conventional PWB with plated-through hole vias (PTHVs) rather than microvias is considered for the board design. Peripheral packages have been adapted to reduce solder joint failures at the die edge as well as to improve routing characteristics of full array plastic packages.

For ceramic packages, however, the need for a peripheral array is less because the CTE mismatch between the die and package materials is negligible. Consequently, most ceramic packages are supplied in full array configuration, including the high I/O CCGA packages evaluated in this investigation. When the ceramic package pad pattern simulates its plastic package version (e.g., the CCGA 560 I/Os), the package may be provided in the form of a peripheral array. In addition, the CCGA 560 I/O package had an interposer with additional solder ball interconnections to the package's land grid array (LGA) pads. This package uses a relatively larger column diameter, possibly to accommodate the heavy weight of the ceramic package and interposer.

This report first presents a survey of key parameters that affect assembly reliability of CCGAs based on a comprehensive literature search, including the effect of tin-lead solder volume on thermal cycle reliability. It also illustrates representative SEM photomicrographs from a previous investigation, showing failure mechanisms for the 560 I/O package assemblies subjected to thermal cycling.

In the experimental study, photomicrographs are presented for two package types, the 560 I/O and a high CCGA, which were successfully recolumned using two column sizes. Tensile strength of column attachment before, during, and after isothermal aging to 500 hours at 125°C were monitored and plotted. Recolumned packages were assembled on printed wiring boards (PWBs) using tin-lead solder pastes that were reflowed either by vapor phase machine or rework station. Details on the key design of test vehicles (TVs) are summarized. Processing parameters and variables used during assembly for the two package types and reflow processes are documented in details and presented.

The TVs were subjected to three different thermal cycle regimes. Representative optical photomicrographs before and during cycling showing damage progress and failure mechanisms are presented. SEM and cross-sectioning were performed to better define damage type, intermetallic formation, and depth of microcracks. Representative photomicrographs of SEM results were also included. For a high I/O CBGA, representative X-ray photomicrographs of the package after complete separation due to two different thermal profiles showing solder joint failure board are also presented.

3.2 Survey: CCGA Reliability

Table 1 lists cycles to failure for a number of CCGAs having different configurations. It tabulates thermal cycle reliability data for three types of column configurations: pure high melt solder ($Pb_{90}Sn_{10}$), high melt solder ($Pb_{80}Sn_{20}$) with Cu spiral, and Cu. The Cu spiral columns are similar to the columns used in package recolumning in this investigation. Key parameters affecting thermal cycling behavior of CCGAs/CBGAs are as follows:

- Thermal cycle range, ramp rate, and dwell times.
- Package size and thickness, including die, materials, configuration, and I/Os.

- PWB thickness, pad definition, and surface finish.
- Single side or double side, and relative offset of package on top and bottom.

Table 1. Cycles-to-failure data illustrating the effect of a number of key variables.

#	Package I/O- Pitch	Pkg Size (die size, mm)	Thermal Cycle Condition (ramp, dwell, cycle/hr)	First Failure	Mean Life (63.2%)	Comments
1	CCGA 472-1.27 Cu spiral column	Not specified	-55°C to 105°C (30 min dwell, 5°C/min)	500 cycles (crack/no failure)		Package size not given Failure definition not IPC 9701 standard Ref [10]
2	CCGA 624-1.27 Cu spiral column	32.5x32.5x2.2 5	-55°C to 105°C (30 min dwell, 5°C/min)	~ 2300	NA	Spiral column showed significantly better TC resistance Ref [11]
3	CCGA 1152 & 1272- 1 mm Cu spiral column	35x35x2.77 & 37.5x37.5x2.7 7	-55°C to 105°C (30 min dwell, 5°C/min)	~ 1200 & 1500		Spiral showed improved resistance Ref [11]
4	CBGA937-1.0	32x32x1.5 (substrate) 32x32x2.4	0°C to 100°C (2 cycles/hr)	NA	1860 (N _{50%}) 1310 (N _{50%})	Ref [12]
5	CCGA 1144-1.0 90/10 Pb/Sn column	35x35x1.59	0°C to 100°C (2 cycles/hr)	No Failure to 5000 cycles	NA	Ref [13]
6	CCGA1657-1.0 90/10 Pb/Sn	42x42x1.5 42x42x2.55 42x42x3.7	0°C to 100°C (2 cycles/hr)	NA	1530 (N _{50%}) 990 620	Ref [14]
7	CCGA 1657-1.0 Cu column	42.5x42.5x 2.55	0°C to 100°C (2 cycles/hr)	1660 (1 st failure)	2410 (N _{50%})	Cu column, solder paste 96.5 Sn3.5Ag Ref [15]

3.3 Effect of Solder Joint Volume on CCGA Assembly Reliability

In contrast to PBGA assemblies, the reliability of CCGA and CBGA assemblies is significantly affected by the amount of solder volume. In fact, solder volume is the most important key process variable affecting the reliability of CCGAs/CBGAs. Recommended minimum, optimum, and maximum solder paste volumes for both CBGA and CCGAs are shown in Table 2 [16], [17]. As one might expect, higher solder volume for CBGAs increases the solder balls' standoff height, which affects reliability. However, this is not the

case for the CCGA assemblies where the effect is more complex in that column flexibility also plays a role in reliability.

For CBGAs, increasing solder paste volume increases reliability, but only up to a point. When the paste volume passes 10,000 cubic mils (0.16 cubic mm), the reliability no longer increases because the solder paste has filled the area between the ball and the card. Additional solder paste moves the ball up toward the module, making the ball look like a column. When the fillet dimension at the card surface is maximized, so is the reliability.

Unlike CBGAs, CCGA assemblies may show a decrease in solder joint thermal cycle reliability at higher solder volumes. As the solder volume increases, so does the fillet height on the column. The increased fillet height reduces the effective length of the flexible column, making it stiffer. This effect—while true for both cast and wire—is more pronounced for the cast because it is stiffer due to its larger diameter [17]. In a comprehensive investigation performed for this category of packages [17], it was shown that assemblies with a minimum acceptable solder paste exhibited slightly higher reliability than those with nominal solder paste, and much better than those with higher solder volume. To avoid inducing opens, however, the use of nominal rather than minimum solder paste volume is recommended.

Table 2. Solder paste recommendation for CBGA and CCGA, 1.27 mm pitch.

Component Type	Minimum Paste Volume mil ³ (mm ³)	Optimal Paste Volume mil ³ (mm ³)	Maximum Paste Volume mil ³ (mm ³)
CBGA	4800 (0.089)	6500-7500 (0.10-0.20)	10000 (0.160)
CCGA	3000 (0.0470)	5000-5600 (0.078-0.088)	7600 (0.120)

3.4 Failure Mechanisms of CCGA 560 I/Os

In a previous investigation [1], thermal cycle behaviors of CCGA 560 I/Os with interposer were established. Figure 5 depicts SEM photomicrographs and cross-sections of the CCGA assemblies after cracking due to thermal cycling. Note the relatively large columns with interposer between package and column attached by solder bumps through the interposer thickness cavity. Even though no outright failures were observed, solder joints exhibited signs of damage both at the board and within the interposer. This makes it difficult to project failures based on solder joint behavior at the board, visually inspected during thermal cycling. For an assembly with a high solder volume, the first failure is shown to occur at the package side, detected by continuous monitoring. Also, failures more commonly occur at the board side for CCGAs with no interposer. For assemblies with lower solder volumes, solder joints exhibited more damage at the board side rather than the package side. Failures were from solder joints at the board side for the lower volume condition.

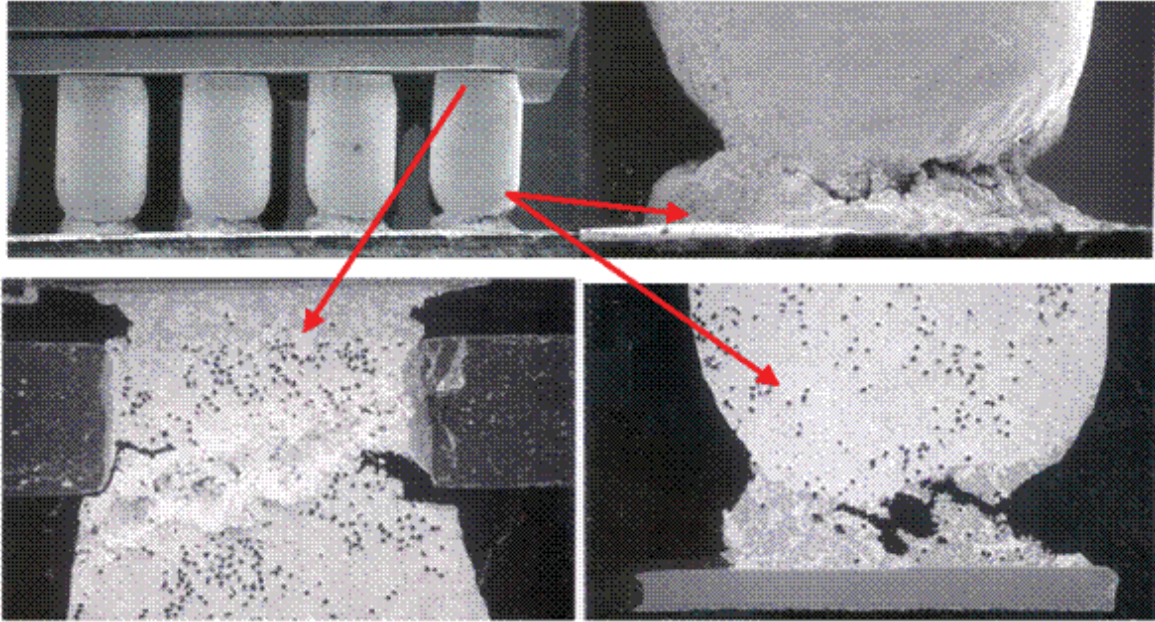


Figure 5. SEM photomicrographs and cross-sections of CCGA 560 I/Os assembled with tin-lead solder after thermal cycling showing damage/cracks.

3.5 NASA and Industry Standards for Assembly, Rework, and Thermal Cycle

Even though there are no unique specifications for rework and assembly of CCGA, numerous process controls and specific requirements shall be in place prior to its implementation until such specifications are released. For example, the intent of NASA-STD-8739.3—Soldered Electrical Connections [18], and NASA-STD-8739.2—Workmanship Standards for Surface Mount Technology [19], is applicable. Specifically, SMT techniques and quality assurance (QA) provisions specified in section 7.3—solder paste testing, section 7.4—PWB preparation, chapter 8—materials deposition and parts placement, and chapter 12—QA Provisions of NASA-STD-8739.2 are directly applicable.

Contrary to conventional wisdom, which relies on visual inspection for leaded parts, area array parts can only be partially inspected. Therefore, the key to QA approaches is strong process controls, and then inspection. QA personnel should keep this in mind from the start of assembly until the inspection of peripheral solder joints, subsequent X-ray evaluation, and possible use of C-SAM. In addition, two other key industry IPC specification documents are considered as references: IPC-7711 [20] for rework (sections 3.9.1 and 5.7.2 are for BGA/CSP rework); and IPC 9701 [21] for thermal cycling evaluation.

3.6 Attachment Procedures

To assemble CCGAs, paste deposition was carried out using a number of ministencils, each with an appropriate thickness and aperture opening size to achieve the proper estimated level of solder paste volume. Package placement was accomplished using a split-version rework system. Solder paste reflow was performed using either the rework station or a vapor phase reflow machine. The profile to be used for the rework station was borrowed from a previous activity and tailored, based on additional data from a sample with thermocouple attachment

used while observing melting of solder paste of the outer row of columns during reflow. Reflow profiles for the vapor phase were also based on a previous profile, which was tailored using a sample run with the attached thermocouple. The vapor phase consists of an infrared preheating followed by a constant temperature boiling vapor zone. Infrared preheating temperature/time and time in vapor phase are the only key parameters that can be modified to achieve better solder attachment quality.

3.7 X-ray Characterizations

Real time X-ray systems are categorized as 2-D and 3-D X-ray systems. The 2-D system is a standard X-ray inspection system with a microfocus source and a stationary image intensifier as the detector, capable of producing offset pseudo 3-D features [21]. The second 2-D system is an X-ray tool with a similar microfocus source intensity and stationary position, but the detector has off-axis rotational capability. The transmission X-ray captures everything between the X-ray source and image intensifier since X-rays are emitted from the source and travel through the sample. The higher the density of the sample, e.g., columns in CCGAs, the fewer X-rays pass through and are captured by the image intensifier. The detected X-rays are displayed in a grayscale image, with the lower density areas, such as voids, appearing brighter than the higher density areas. The voltage and current of the X-ray's intensity can be adjusted to reveal features in most sections of the sample.

The 2-D X-ray systems are very effective in testing single-sided assemblies. With the use of a sample manipulator, an oblique view angle enhances inspection of both single- and double-sided assemblies with some loss of magnification due to increase in distance between source and detector. Experience is needed in discerning between bottom-side board elements and actual solder and component defects. This can be very difficult or even impossible on extremely dense assemblies. In any case, only certain solder-related defects such as voids, misalignments, and solder shorts are easily identified by transmission systems. However, even an experienced operator can miss other anomalies such as insufficient solder, apparent open connections, and cold solder joints.

The X-ray system with a rotational detector allows oblique generation of X-ray images with a higher magnification and a better intensity resolution since the focal spot remains the same and, therefore, there is no loss of magnification. An isocentric manipulator keeps the field of view unchanged when the oblique view mode is used. This feature allows better characterization of some defect features, including wettability and void location in area array packages.

3.8 Scanning Electron Microscopy Characterizations

Scanning electron microscopy (SEM) with variable pressure (VP) and low vacuum (LV) is generally used for imaging materials with low atomic numbers such as polymers. The beam-specimen interaction volume, together with low backscatter electron coefficients, determines the ultimate spatial resolution and image quality. A proficient variable pressure secondary electron detector is essential for high resolution. The compositional images presented under SEM evaluation were obtained with a LEO Supra-50 VP, field-emission tungsten source. The SEM is capable of secondary electron imaging and backscatter electron imaging under all pressures and conditions. The specimens are imaged at

pressures between 30 and 133 Pa (0.3-1 torr) to achieve charge compensation even though fluxes still showed charging, imaged as dark areas.

3.9 Thermal Cycle Profiles

Three different cycles were used with the following thermal profiles for thermal cycle characterization of CCGA assemblies:

1. Cycle A: Ranged from -55° to 100°C with a 2° to $5^{\circ}\text{C}/\text{min}$ heating/cooling rate. Dwells at extreme temperatures were 15 minutes.
2. Cycle B: Ranged from -55° to 125°C with a 2° to $5^{\circ}\text{C}/\text{min}$ heating/cooling rate. Dwells at extreme temperatures were at least 10 minutes with duration of 159 minutes for each cycle.
3. Cycle C: Ranged from -120° to 85°C with about $5^{\circ}\text{C}/\text{min}$ heating/cooling rate and 10 minute dwells.

4. Experimental Approaches—Recolumn of CCGA 560 I/Os

4.1 Purpose for Using CCGA 560 I/Os

The first part of the investigation concentrated on understanding rework of a large, 42.5-mm CCGA package with interposer having a thermal cycling behavior that was well characterized in a previous investigation [1], [2]. Figure 6 depicts a photomicrograph of this package with interposer attached and its interposer layer alone. The CCGA 560 I/Os package had a few key characteristics that were ideal for the rework/recolumn/reassembly process and reliability optimization, including:

1. Individual virgin packages as well as TVs with package assemblies were available, and the effect of additional rework on thermal cycle behavior after recolumning/reassembly could be compared.
2. The package had an added interposer for absorbing CTE mismatch to improve solder joint reliability. This thin ceramic interposer was removed prior to recolumning.
3. Possibly because of the package size and interposer, solder column diameters are larger than recolumned diameters; therefore, the recolumned version requires smaller PWB pad sizes.
4. The ceramic package is relatively large since it simulates its plastic counterpart package with the identical configuration, I/O counts, and 1.27-mm pitch. It is a peripheral array rather than a full array package.
5. Two pad designs were considered in the initial TVs, one for CCGA and the other for PBGA. Both were utilized for recolumned packages.

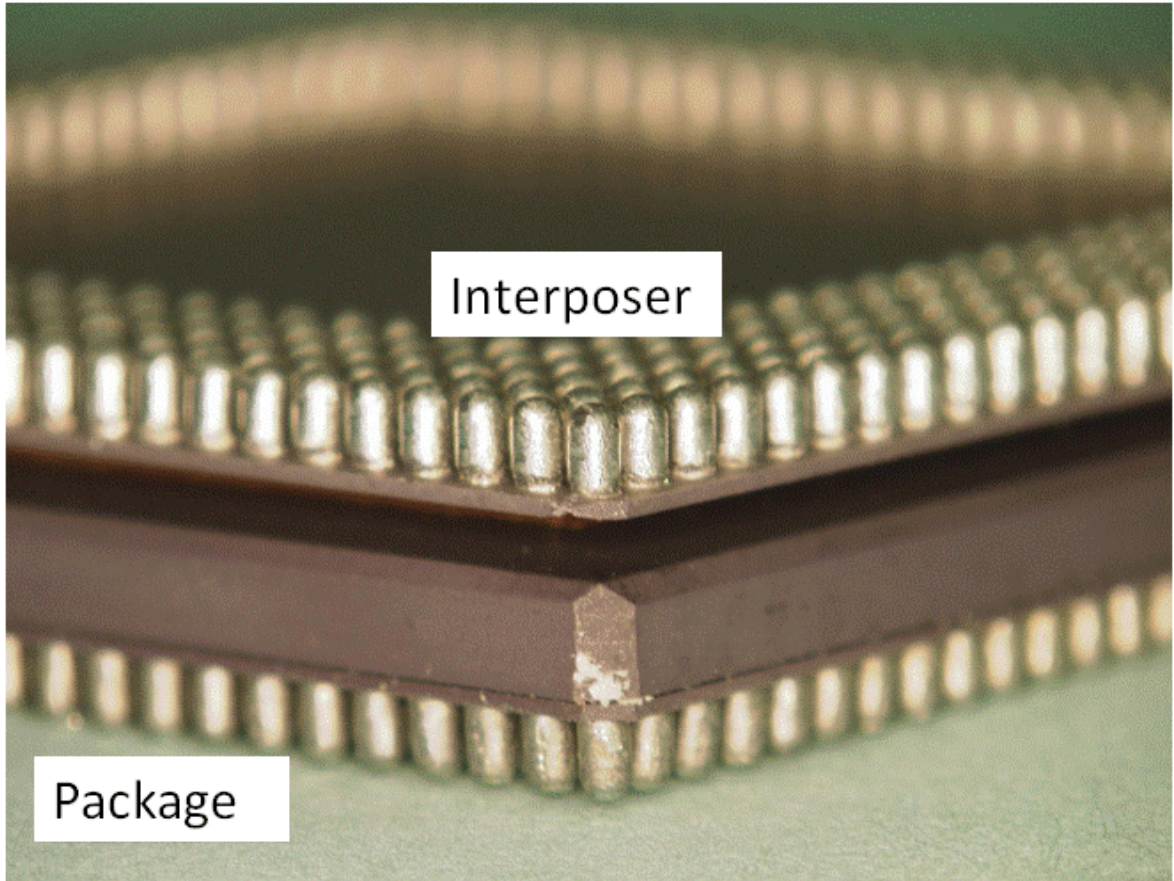


Figure 6. Optical photomicrograph of a virgin CCGA 560 I/O package before recolumning with interposer (bottom) and an interposer layer alone on the top.

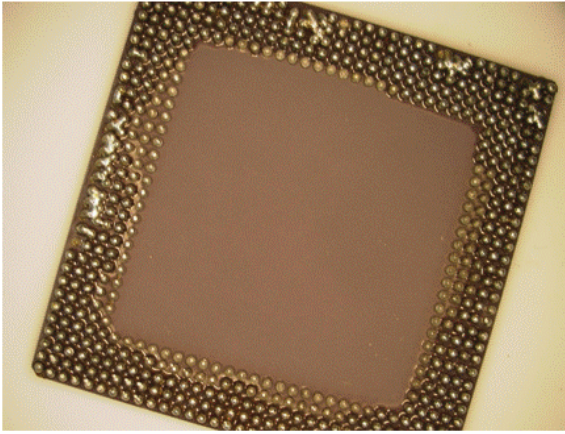
4.2 Key Rework, Recolumn, and Reassembly Parameters for 560 I/Os

A design of experiments (DOE) technique was utilized to cover many aspects of recolumning/reassembly that are considered unique for this package configuration. The following parameters were part of the DOE even though, in some cases, because of reassembly, processing issues could not be fully evaluated for subsequent thermal cycling behavior characterization.

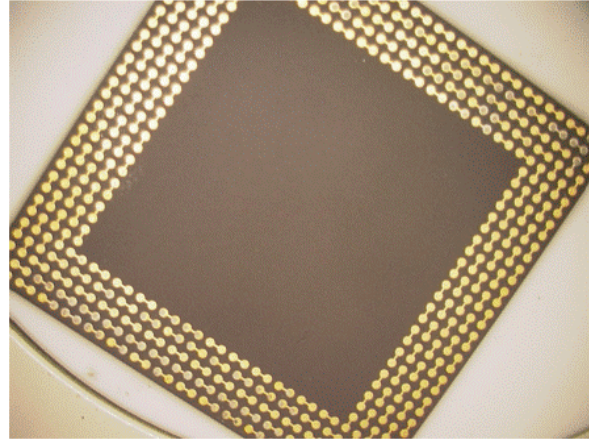
- CCGA packages with and without corner staking were successfully removed from assembled TVs. In the first attempt, corner stakes induced minor damage to the board at corners away from the pads since the direction for removal was not clearly specified. This issue was corrected in subsequent removal, and damage to boards was minimal. Figure 7 depicts photomicrographs of packages after removal where remnants of corner staking materials are apparent. Solder columns remain on the package interposer after package removal, and package pad daisy chain patterns became apparent when the interposer layer was removed.
- Interposer layers were removed both for virgin and reworked packages prior to recolumning of the land grid array package.

- These daisy chain packages had traces between many pads to accommodate full daisy chain resistance monitoring when assembled onto a board. Masking of these traces was considered before recolumning; however, the vendor was able to recolumn the packages successfully without using masking. Tin-lead solder paste was used for column attachment.
- One recolumned virgin package was subjected to pull testing to assure quality of column solder joint attachments prior to committing to recolumning of other parts.
- Two additional recolumned virgin packages were subjected to isothermal aging and pull testing to determine quality of bond interfaces after aging exposures. One package had an additional simulated recolumning reflow to represent rework.
- Two ministencils were used for the two pad sizes: one designed for CCGA pads, and the other designed for smaller pads for PBGA attachment. Mostly the CCGA pad design was used.
- All packages were placed onto PWBs using a rework station. Both the rework station and the vapor phase reflow machine were used for reflowing solder pastes. The TVs with PBGA assemblies were also reflowed in place one more time during reflow of recolumned packages.
- A vapor phase reflow profile for tin-lead solder with constant reflow temperature at 217°C for 60 seconds was used.
- Acceptable reassembled TVs as well as those with known manufacturing defects were subjected to thermal cycling to detect early failures due to workmanship and damage progress with cycling for parts with acceptable quality.
- Optical photomicrographs, X-ray, and cross-sectioning were documented.

Package pull tests before and after isothermal aging and reliability test results for CCGA package assemblies are discussed in detail in the following section.



Reworked Package



Package Base

Figure 7. Optical photomicrographs of a removed CCGA 560 I/O package after rework showing removed/shorted columns (left) and package daisy chain pattern without interposer (right).

4.3 Pull Strength Cu Spiral Columns Attachment Pre- and Post-Aging

Recolmned packages were subjected to pull testing to determine the strength of Cu spiral columns and attachments. A small solid cylinder with a diameter of a few columns was attached to a column (~22 mils) and subjected to pull testing. Load values and failure modes were recorded. Table 3 summarizes values for a number of columns that were pull tested. It also includes failure modes; all had ductile failure of the columns with no failures at the attachment interconnections. The average force was 1340 g with standard deviation of 137 g, a very consistent column quality since no interfacial failure was observed.

Table 3. Summary information of a representative column's pull-test results.

Column Pull Test

Background:
Column pull test is a method used to determine the strength of the attached column interconnects and the corresponding failure mode. This test yields quantifiable data that pertains to the quality and consistency of the solder column, fillet, and pad. Column pull is a destructive test.

Failure Modes:

Mode 1 Column Failure – Failure through the core of the wire, leaving the copper wire spiraling out away from the fractured core (see Figure 1).

Mode 2 Joint to Pad Failure – Failure of the column attach joint on the device side. Non-solder colored material must be visible on the device side of the fracture. Probable causes: pad contamination, pad corrosion or excessive intermetallic growth.

Mode 3 Pad Failure – Pad is lifted off from the device substrate.

Mode 4 Fixture Failure – Failure is through or at the fixture attach joint.

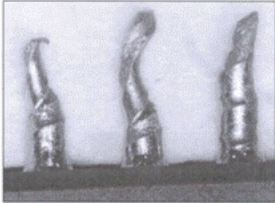


Figure 1. Failure mode 1 for reinforced column.

Column Diameter
 $6=0.086''$, $5=0.087''$, $1=.081''$

Pull Test Report

Date: 07/05/07	
Sales Order: 56771	
Customer: Jet Propulsion Laboratory	
Part Type: CCGA 560L-50-87-22	
Part Number: CG 560 DAISY CHAIN	
Prepared By: M. Cruz	<input checked="" type="checkbox"/> Pass <input type="checkbox"/> Fail
Pull Speed: 1.0 inch/minute	
Equipment: Digital Force Gauge Cal. # 185	
Comments: Test performed in accordance with TS-3012: Operation of Pull Tester	

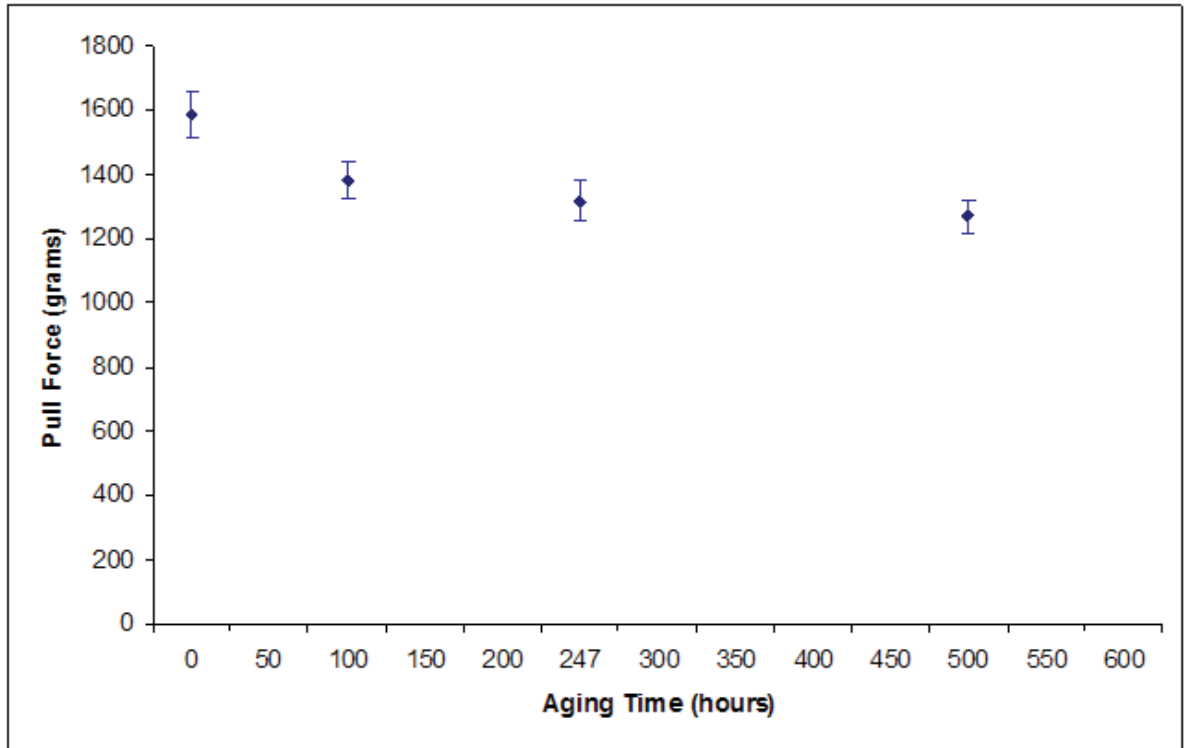
Measurement #	Peak Force (g)	Failure Mode
1 (periphery)	1380	1
2 (periphery)	1384	1
3 (periphery)	1301	1
4 (periphery)	1140	1
5 (periphery)	1148	1
6 (periphery)	1375	1
7 (periphery)	1298	1
8 (periphery)	1646	1
9 (periphery)	1097	1
10 (periphery)	1411	1
1 center	1345	1
2 center	1343	1
3 center	1441	1
4 center	1439	1
5 center	1345	1

Average Peak Force: 1340
 Standard Deviation: 137

Pull Peak Force = 1340 g
Standard Deviation = 137
Failure- Column (mode 1)

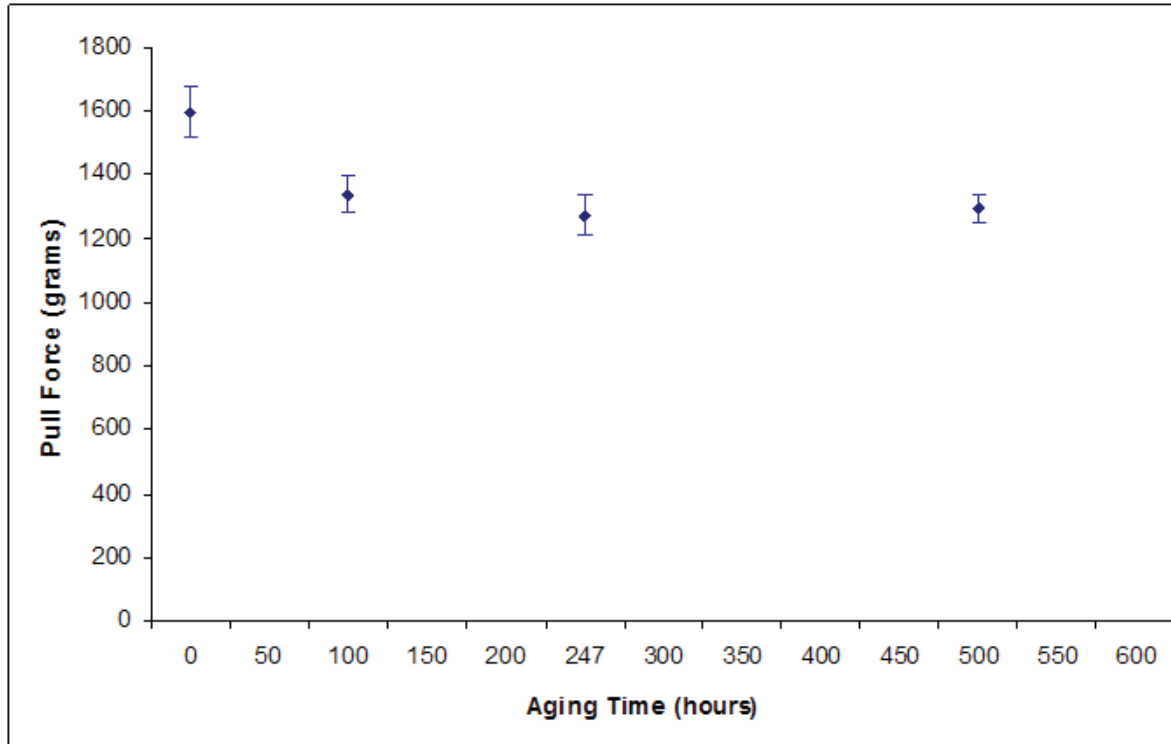
One key concern is interconnection degradation due to high temperature exposure during assembly and application. During assembly, recolumned packages are exposed to one additional reflow cycle, whereas as-assembled packages are exposed only to one reflow if no reworking is allowed. The effect of this additional reflow on interfacial intermetallic growth is unknown and may be significant. This effect was considered by performing one additional reflow prior to long-term, high temperature exposure. Exposure was performed at 125°C on two recolumned packages, one with an additional reflow cycle, for a total of 500 hours. Pull testing was performed at 100, 247, and 500 hours of aging to determine degradation with time.

The average pull-strength variations with time for two conditions are shown in Figures 8 and 9. Pull strength values decreased rapidly initially and then slowed down with time, for a total decrease of 19% at 500 hours. Comparing the two figures, it is apparent that degradation due to a pre-reflow cycle prior to aging is negligible. It was discovered that the reflow cycle performed at the vendor was less than five seconds, much lower than the 45–90 seconds generally used during assembly. Therefore, shorter reflow this time may not be fully representative of typical reassembly conditions.



Aging Time (hours)	Average Pull Force (grams)	Standard Deviation (grams)
0	1585	70
100	1383	56
247	1316	62
500	1270	49

Figure 8. Pull strength decrease with isothermal aging at 125°C for 500 hours for the reconstituted 560 I/O package.



Aging Time (hours)	Average Pull Force (grams)	Standard Deviation (grams)
0	1598	80
100	1338	57
247	1273	64
500	1294	41

Figure 9. Pull strength decrease with isothermal aging at 125°C for 500 hours for the 560 I/O recolumned package with an additional column-attachment reflow cycle.

Optical photomicrographs of solder column attachment after exposure at 125°C for 500 hours are shown in Figures 10 and 11. Shown are minor microstructural changes that are more pronounced for the solder joints exposed to an additional recolumning reflow cycle before aging. Failures under all three conditions—as built, no reflow, and one reflow cycle—were from columns rather than within solder or at the interface between solder and pad.

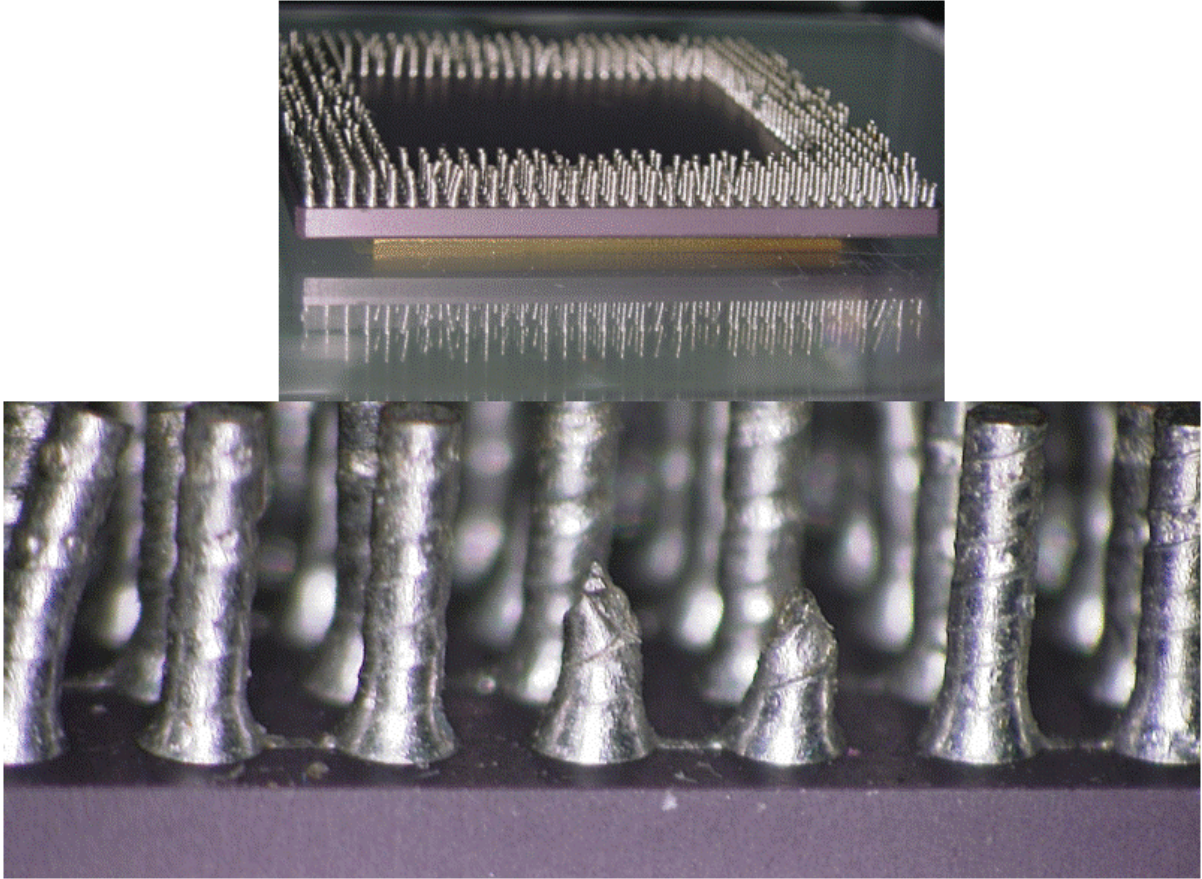


Figure 10. Failure and microstructural changes after 500-hour isothermal aging at 125°C.

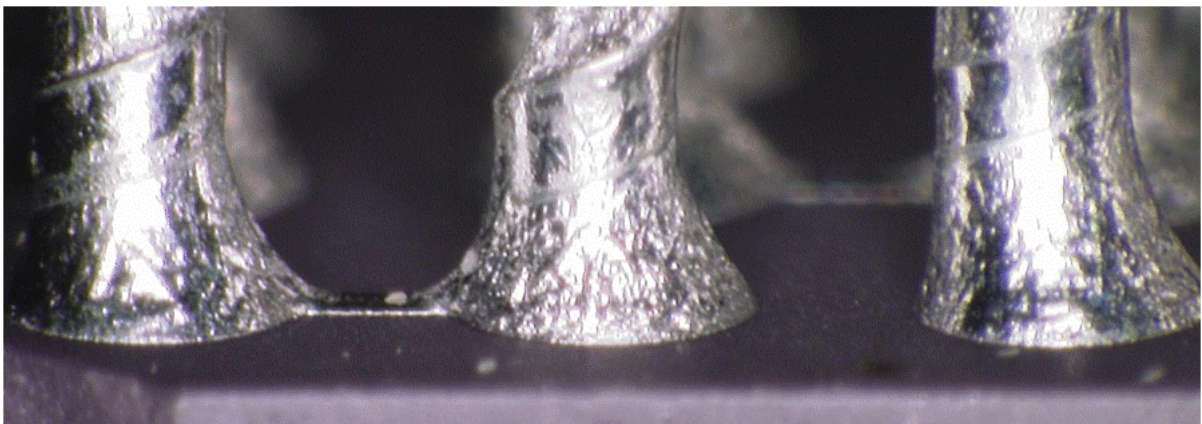


Figure 11. Failure and microstructural changes after one reflow cycle and subsequent 500-hour aging at 125°C.

The vendor report on column strength characterization is provided in section 11. It documents details of test procedure and the individual pull test results for the two 560 I/O recolumned packages. It also includes interpretation of test data by the vendor as provided. Note that column alloys for a number of columns were measured at the vendor facility by X-ray Fluorescence (XRF) and were tabulated. The Cu spiral columns solder alloy

reported as $Pb_{80}Sn_{20}$ composition is different as determined from XRF. It also has slightly lower lead content than the standard solder column with Pb_{90}/Sn_{10} solder alloy composition.

4.4 PWB/TV/Package CCGA 560 I/Os

Figure 12 depicts the top and bottom of the board design for the CCGA 560 I/O package assembly showing the daisy chain configurations, including PBGA 560 I/Os, probing pads, and PTHVs. Polyimide printed wiring boards (PWBs) were designed to accommodate two pad configurations, one for the PBGAs and the other for the CCGAs. Polyimide rather than FR-4 PWB is commonly used for high reliability applications. The pad sizes for the PBGA and CCGA were 24 and 33 mils, respectively.

The traces from the pads were attached to PTHVs with a 24-mil diameter. Specific pairs of pads were connected through PTHs; these connections within a package pair complete the daisy chain patterns, enabling solder joint continuity monitoring during various environmental testing. Four key daisy chains for each package were used for continuous monitoring during thermal cycling. Four additional pads were added at each side of the package for manual probing and failure identification. The probing pads were used when an overall failure was detected through continuous monitoring.

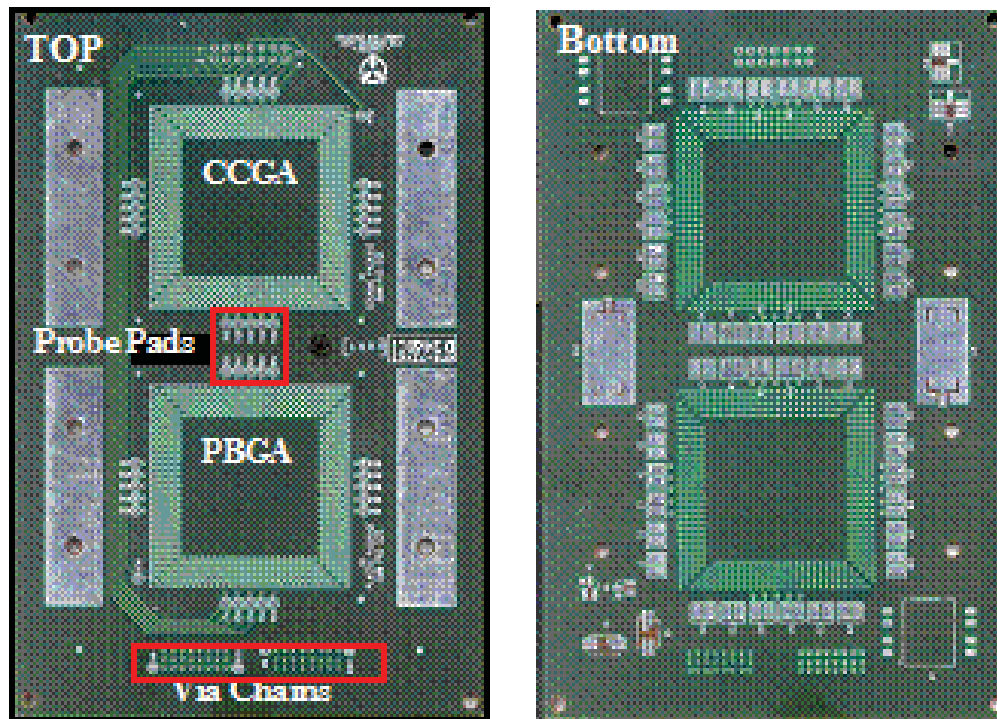


Figure 12. PWB design showing package daisy chain, probing pads, and via daisy chains.

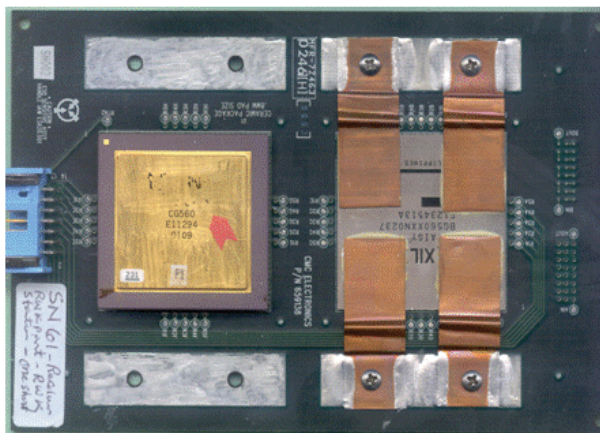
The PWB's pads had Hot Air Solder Level (HASL) surface finish. HASL and Organic Solderability Preservative (OSP) surface finishes are specified in IPC-9701A [21] as the recommended surface finishes for tin-lead solder attachment thermal cycle reliability evaluation. The key reason for such recommendation is to avoid potential premature

intermetallic failures such as those occasionally observed for the electroless nickel immersion gold (ENIG) surface finish.

4.5 Recolumn and Reassembly of CCGA 560 I/Os

A detailed test matrix for rework, recolumn, and reassembly of TVs was outlined at the start of the build. However, during subsequent reassembly, it was recognized that on-the-spot modifications are required to achieve acceptable assemblies based on visual inspection. Figure 13 includes two representative TVs after reassembly of recolumned CGA 560 I/O packages. One has acceptable quality, but the other was rejected because it was observed that gross package twisting had occurred possibly due to uneven heat flow by the rework station during reflow. Instructions initiated at the start of build and changes as assembly process progressed for various TVs are summarized below.

- Remove CCGAs from assemblies of SN02, SN12, and S13 and call them P1, P2, and P3 respectively. Add 12 more virgin parts and send for recolumning.
 1. Subject one recolumned package to pull test to establish baseline.
 2. Subject one recolumned package to additional reflow process after recolumn.
- Subject item 2 and one more recolumned package to isothermal aging. Perform pull test before and after environmental aging. Document test results.
- Use two ministencils, one with 32 mils (opening)/ 8 mils thickness for the ceramic pad patterns and the other with 25/6 mils for the BGA pad patterns.
- Build SN61, SN62, and SN63 using previously reworked SN02, SN12, and S13, respectively. Use rework station and 32 mils/8 mils thickness stencil. Inspected SN62, one short outer column. SN62, assembly visually acceptable. SN63, part rotated and reject.
- Build SN64, 32/8 stencil, rework station. One side no reflow of solder paste. Use vapor phase reflow since inspection showed unreflowed solder paste.
- Build SN65—one part only, large pad use 32 mil/8mil mini stencil, vapor reflow 280, 140, and 60—acceptable.
- SN66—two parts, large pad use 32 mil/8mil mini stencil, left 25 mil/6 mil stencil.
 1. SN 66A P7 part assembled on ceramic pad using 32/8 mil, 280 140, 60—relatively acceptable.
 2. SN 66B P8 part using 25/6 mils on BGA pad, vapor reflow 32/8 mil 280, 140, 60 sec. Reject, many columns shifted.
- SN 67—two parts, large pad use 32 mil/8mil mini stencil, left 25 mil/6 mil stencil.
 1. SN67A use P9 on PBGA pad 32/8 mil, vapor phase 280, 240, 60 sec., Reject column shift/short.
 2. SN67A use P10 on ceramic pad 32/8 mil, vapor phase 280, 240, 60 sec., Reject column shift/short.
- SN 68—two parts, large pad use 32 mil/8mil mini stencil, left 25 mil/6 mil stencil. SN68—(previous SN020 with BGA heat strap) only one part, P12, ordered new stencil 32/8 mil, vapor phase 270, 140, 30 sec., Acceptable.
- SN69, SN70, SN71 using P11, P12, and P13 parts, respectively. Ordered new stencil, 32/8 mil, vapor phase 270, 140, 30 sec. All three considered to have acceptable quality.



Recolump/Rework- Accept

Recolump/Rework- Reject

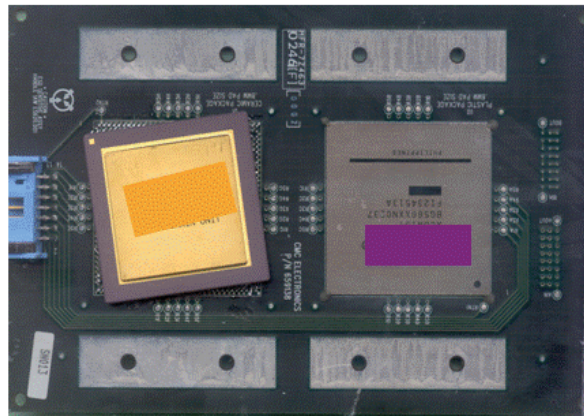


Figure 13. Representative TVs after reassembly of recolumped CGA 560 I/O packages: one with acceptable quality and the other rejected with gross package twisting occurring during solder reflow using a rework station.

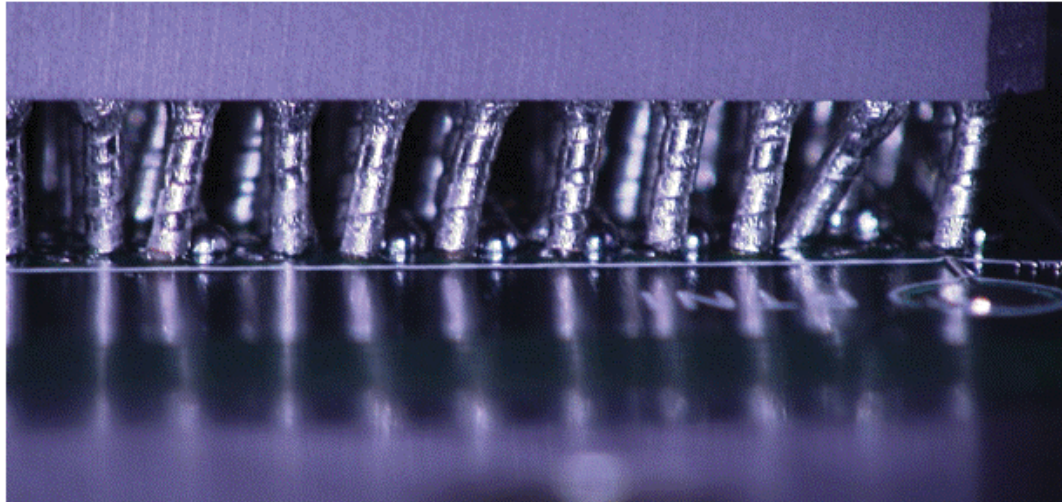
4.6 Inspection after Reassembly

Photomicrographs were taken after all test vehicles were reassembled to document quality of solder joints, including those with various workmanship defects. Figures 14 and 15 are representative of optical photomicrographs for recolumped 560 I/O packages assembled under various conditions. Several processing defects are noticeable from these photos, including the following:

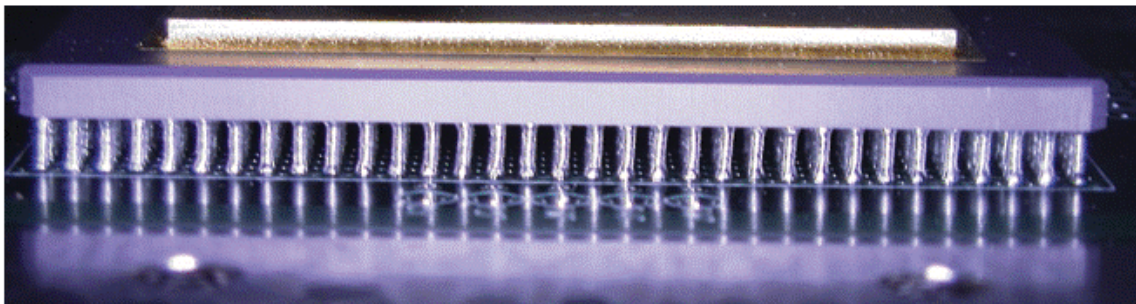
- Photomicrographs comparing quality of solder joints reflowed by vapor phase machine or rework station. In a case where solder paste was not reflowed by rework, station was reflowed using reflow machine.
- Significant column shift when the package is assembled on relatively smaller pads designed for its PBGA package assembly.
- Solder short between the two columns in the middle of package outer row.
- Corner column shift and also the appearance of solder column separation at the package side (not shown at high magnification).
- Solder balls on the package in addition to the board side; their source was not identified (photomicrographs not shown here).

The soldered column separation from the package side is a significant failure and is unusual. One reason might be the weakness in recolump attachment, which might have been exacerbated by another reflow during reassembly causing solder separation at the pads. Follow-on test results for strength reduction on recolumped packages with and without additional reflow and subsequent aging at 125°C all indicated lack of significant interfacial degradation. Consequently, the tensile test results reject the possibility of failure due to weakness of solder joints at interfaces. Another possibility is that the smaller recolump size relative to the large package size and weight causes elimination of self alignment, which is a key

advantage of the area array package. Daisy chain connections between the pads at the package side also are not representative of a working part and may contribute to such interfacial failure. Solder on daisy chain traces can possibly further facilitate column shifting to the neighboring pads during solder reflow.

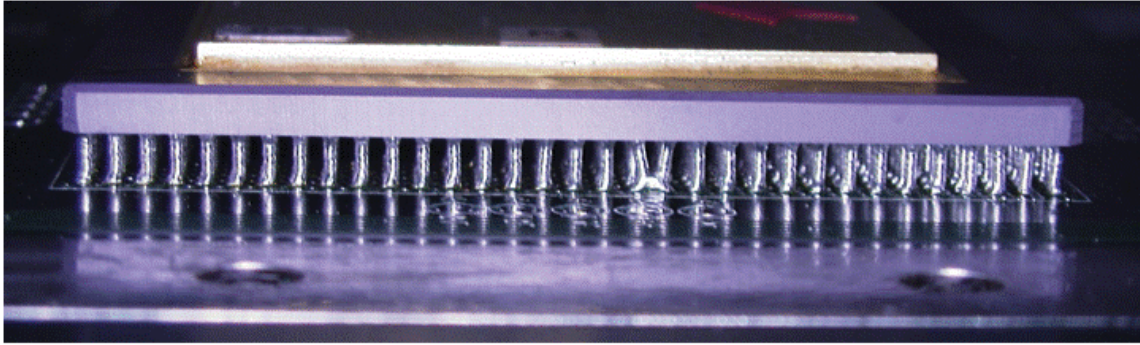


Recolumn-Vapor Phase- On BGA pads

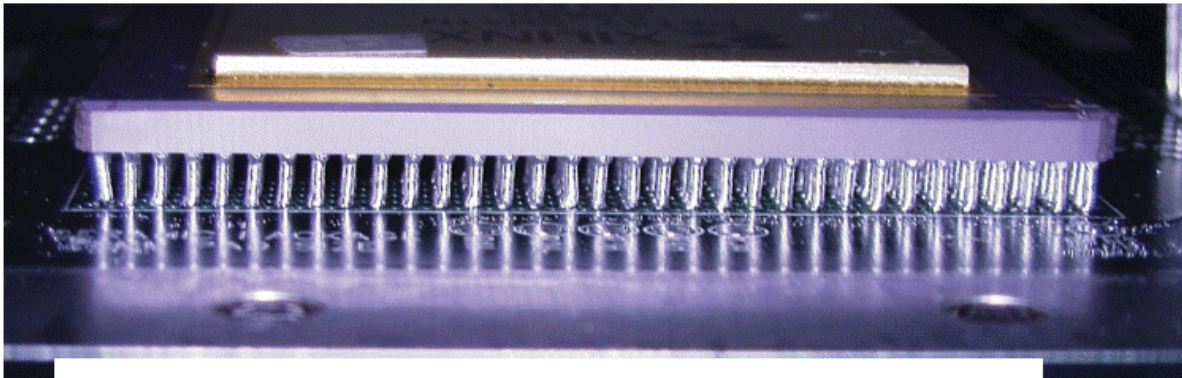


Recolumn-Vapor Phase- CGA Pads- Acceptable

Figure 14. Representative optical photomicrographs for recolumned 560 I/O package reassembly.



Recolumn-Rework Station



Recolumn-Rework Station- Vapor Phase

Figure 15. Representative of optical photomicrographs for recolumned 560 I/O package assemblies.

4.7 Test Results for Recolumned/Reassembled CCGA560 I/Os

4.7.1 Thermal Cycle Conditions

As discussed earlier, because of manufacturing challenges, only a few assemblies had acceptable quality. Four assemblies considered to be acceptable were subjected to Cycle A condition. The Cycle A ranged from -55° to 100°C with a 2° to $5^{\circ}\text{C}/\text{min}$ heating/cooling rate. Dwells at extreme temperatures were 15 minutes.

4.7.2 X-ray Characterization

A real time, 2-D X-ray system with a stationary microfocus source intensity and off-axis rotational capability was used to determine the damage states of recolumned CCGA 560 I/O assemblies. Figure 16 shows an X-ray photomicrograph for an assembled CCGA 560 I/O after thermal cycle exposure. The X-ray technique clearly detects abundance of solder balls but no indication of other defects, neither solder damage nor solder separation at pads due to thermal cycling.

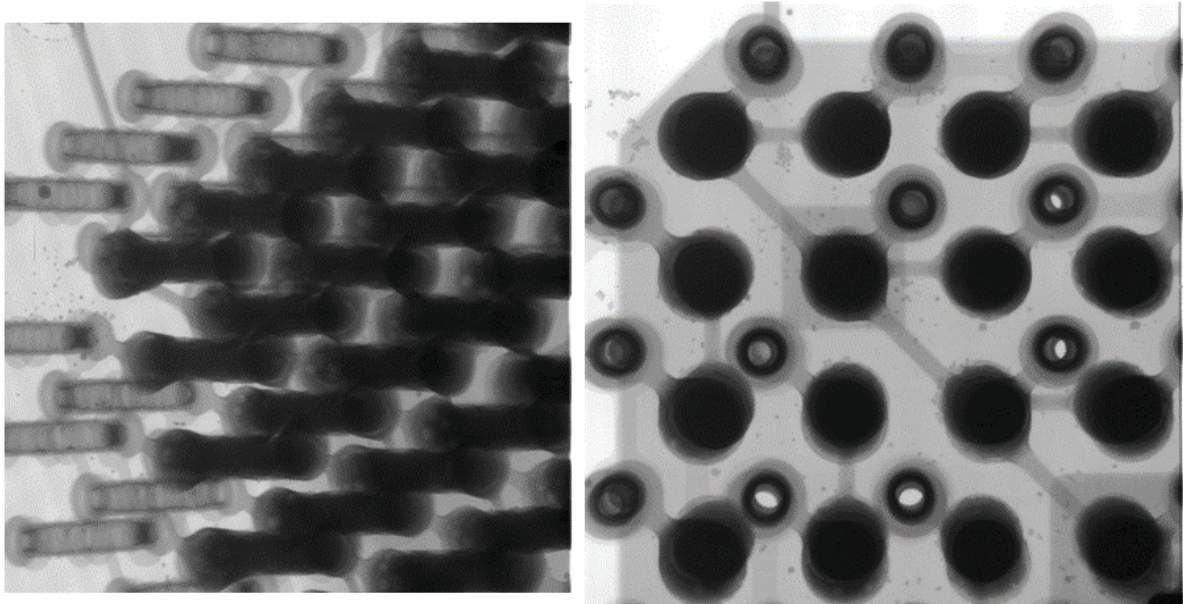


Figure 16. X-ray photomicrograph for recolumned/reassembled CCGA 560 I/Os after thermal cycle exposure showing solder balls, but no separation at package pads detected visually.

4.7.3 Optical Photomicrographs of Damage Progress with Thermal Cycles

Damage progress with thermal cycling was established using optical microscope. Figures 17–19 present representative photomicrographs of workmanship defects and damage due to thermal cycling. Manufacturing defects and damage due to cycling, noticeable from these photomicrographs, can be categorized as follows:

- Solder balls at the package and board sides are apparent from low and high magnifications of column attachments. A large number of solder ball coalescence is shown at the package side at higher magnification. The sources of these solder balls are not clear, but they could be the result of solder splash from paste during solder reflow.
- Several displaced columns showing a larger corner column shift are apparent. Magnified photomicrographs clearly show signs of damage and microcracking due to thermal cycling at the package side.
- Several columns were shifted after thermal cycling. Photomicrographs of these at higher magnification clearly show pad separation from the package. This failure is unusual since microcracking generally occurs in the solder, as shown in the previous figure.

As discussed, soldered column separation from package side is considered an unusual and significant failure. Tensile test results exhibited no such failure mechanisms and no indication of interfacial weakness. Possible reasons for such a failure mechanism may be an unusual package size/weight and use of a smaller-column diameter.

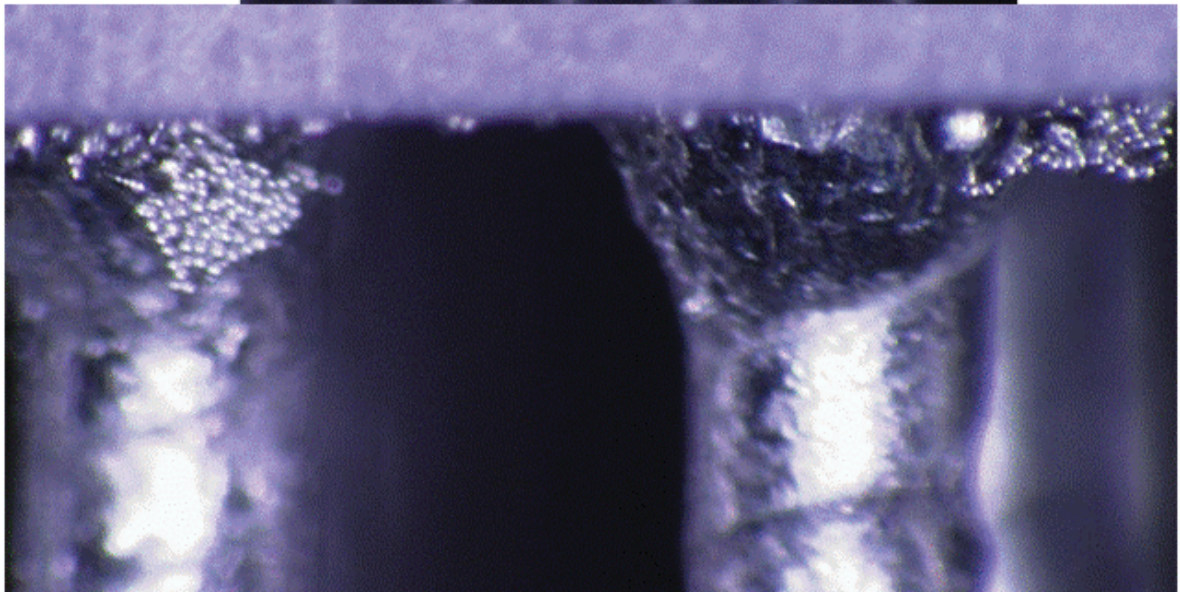
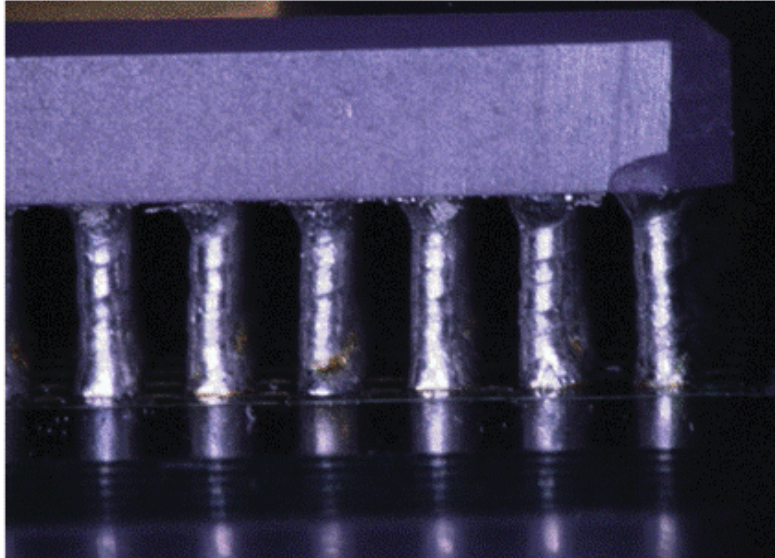


Figure 17. Optical photomicrograph recolumned/reassembled CCGA 560 I/Os after thermal cycles showing solder balls at the package side from manufacturing and solder damage from cycling.

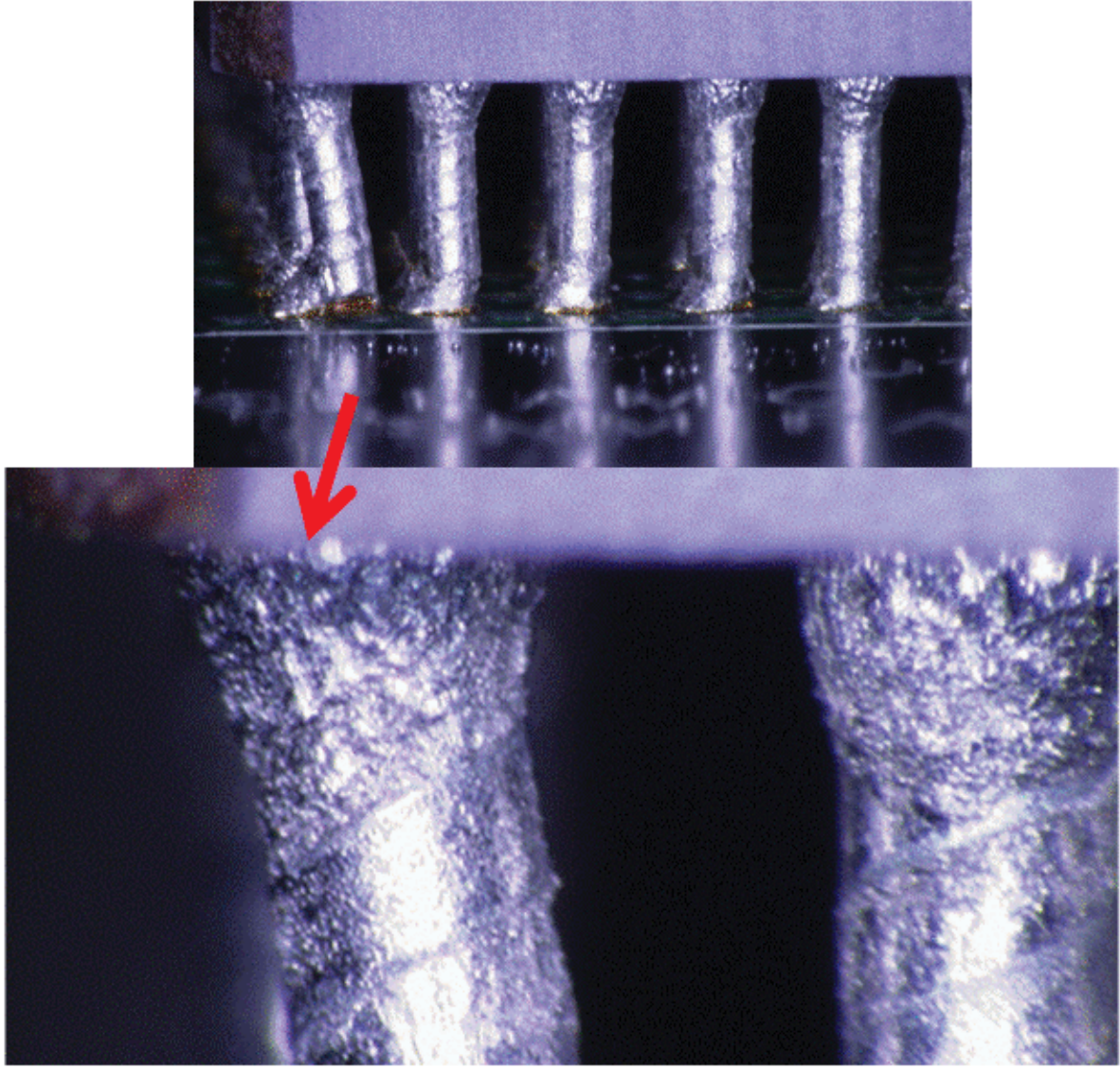


Figure 18. Optical photomicrograph recolumned/reassembled CCGA 560 I/Os after thermal cycles showing microcracks in solder at the package side.

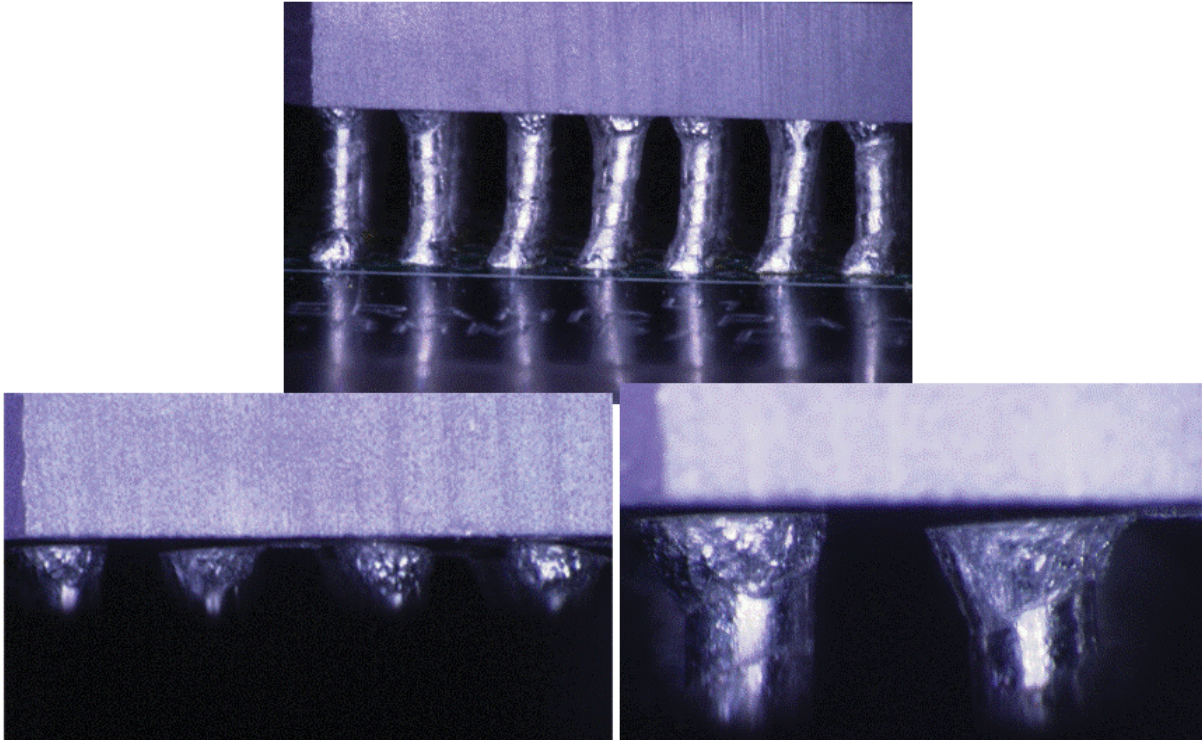


Figure 19. Optical photomicrograph recolumned/reassembled CCGA 560 I/Os after thermal cycles showing solder separation at the package side.

4.7.4 SEM Photomicrographs and X-section

After thermal cycle completion, one sample was cut at its periphery in preparation for additional optical, SEM, and cross-sectioning. Figure 20 depicts representative optical photomicrographs of the assembly prior to cross-sectioning. Damage and microcracks exhibit better resolution since optical lenses now can get close to the package with no interference from the board. Figure 21 depicts representative SEM backscatter photomicrographs of column attachments at various magnifications up to 1,000 times. Cracks at the package side in solder interfaces are clearly apparent. Figure 22 depicts a photomicrograph at much higher magnification showing at least three types of microcracks. Potential mechanisms include: a) the large microcracks at the package interface surrounding the pad interface are due to the weak recolumn attachment; b) the microcracks close to Cu spiral are due to weak Cu/solder interface; and c) the microcracks parallel to interface between solder and column are due to the overall package/board CTE mismatch.

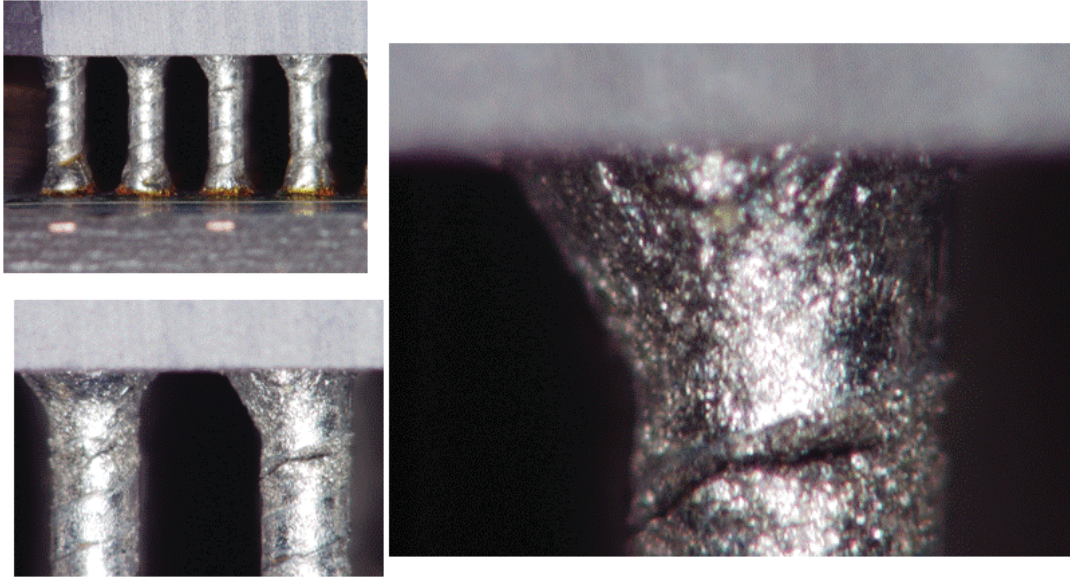


Figure 20. Optical photomicrographs of recolumned/reassembled CCGA 560 I/Os after thermal cycles and prior to X-sectioning showing microcracks in columns and solders at the package side.

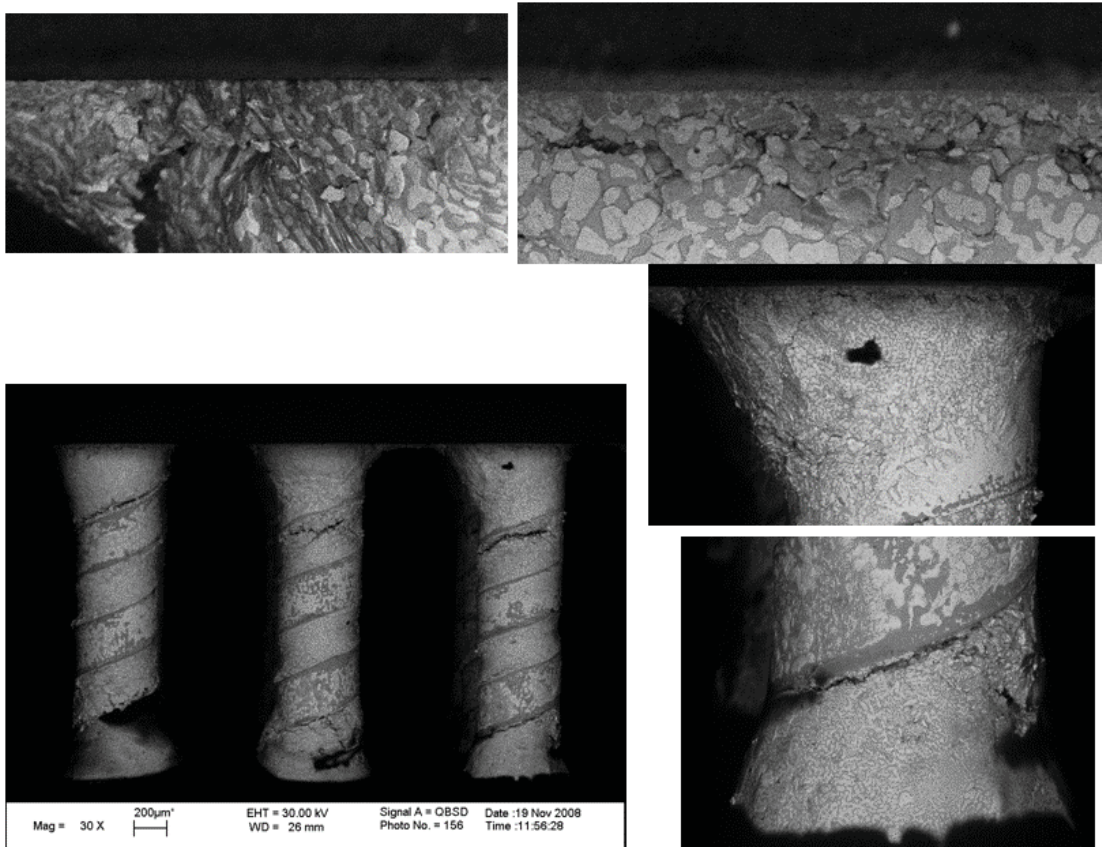


Figure 21. SEM photomicrographs of recolumned/reassembled CCGA 560 I/Os after thermal cycles and prior to X-sectioning showing microcracks in columns and solders at the package side.

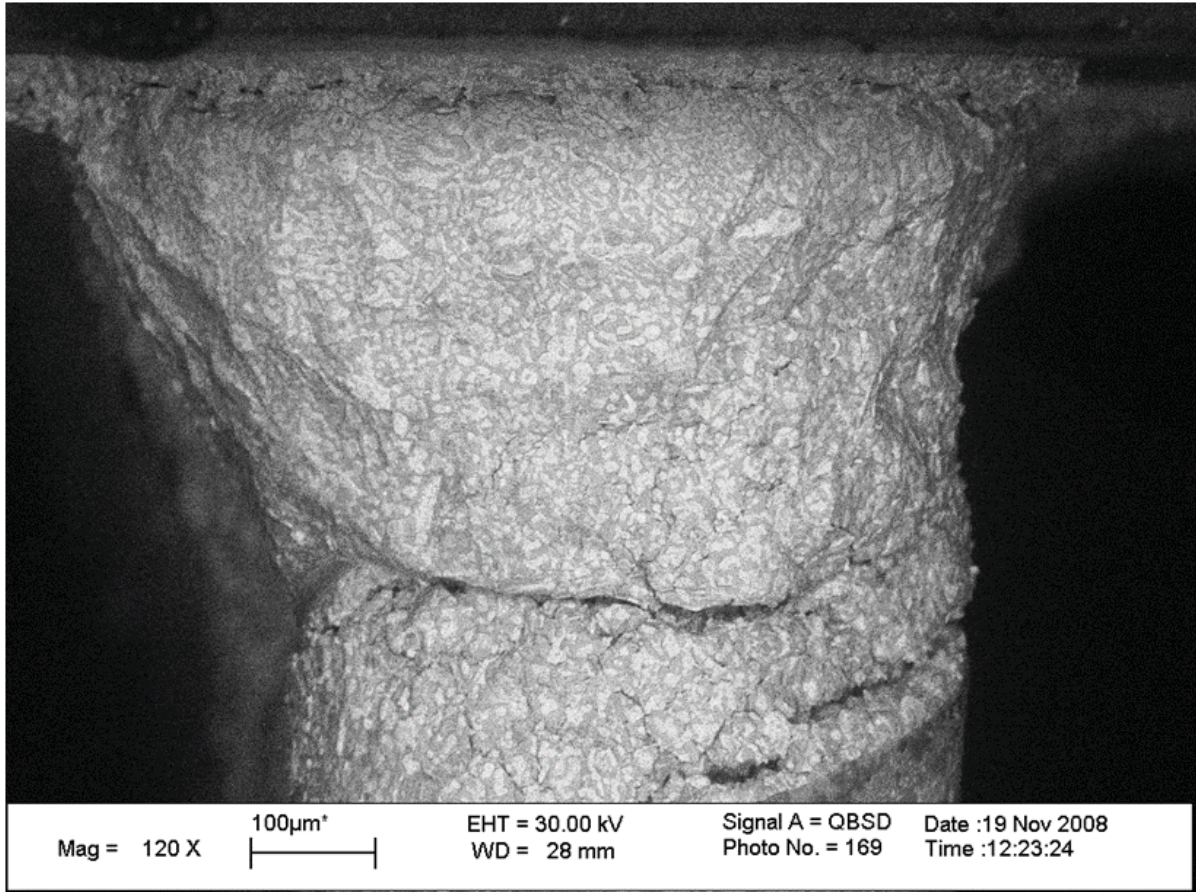


Figure 22. SEM photomicrograph of recolumned/reassembled CCGA 560 I/Os after thermal cycles and prior to X-sectioning showing different types of microcracks in column and solder at the package side.

X-section photomicrographs for the three corner columns are shown in Figure 23. It clearly shows significant damage and minor-to-full cracking, more often at the package sides. Figure 24 depicts SEM photomicrographs at higher magnifications, showing interfacial damage conditions both at the package and at the PWB sides. Separation at the package pad interface with minimum solder remnant at the pad is possibly an indication of weaker metallurgical bond due to recolumning and second reflow. More damage and cracking at the package side may also be due to a larger local CTE mismatch between the ceramic package and solder in comparison to polymeric PWB and solder.

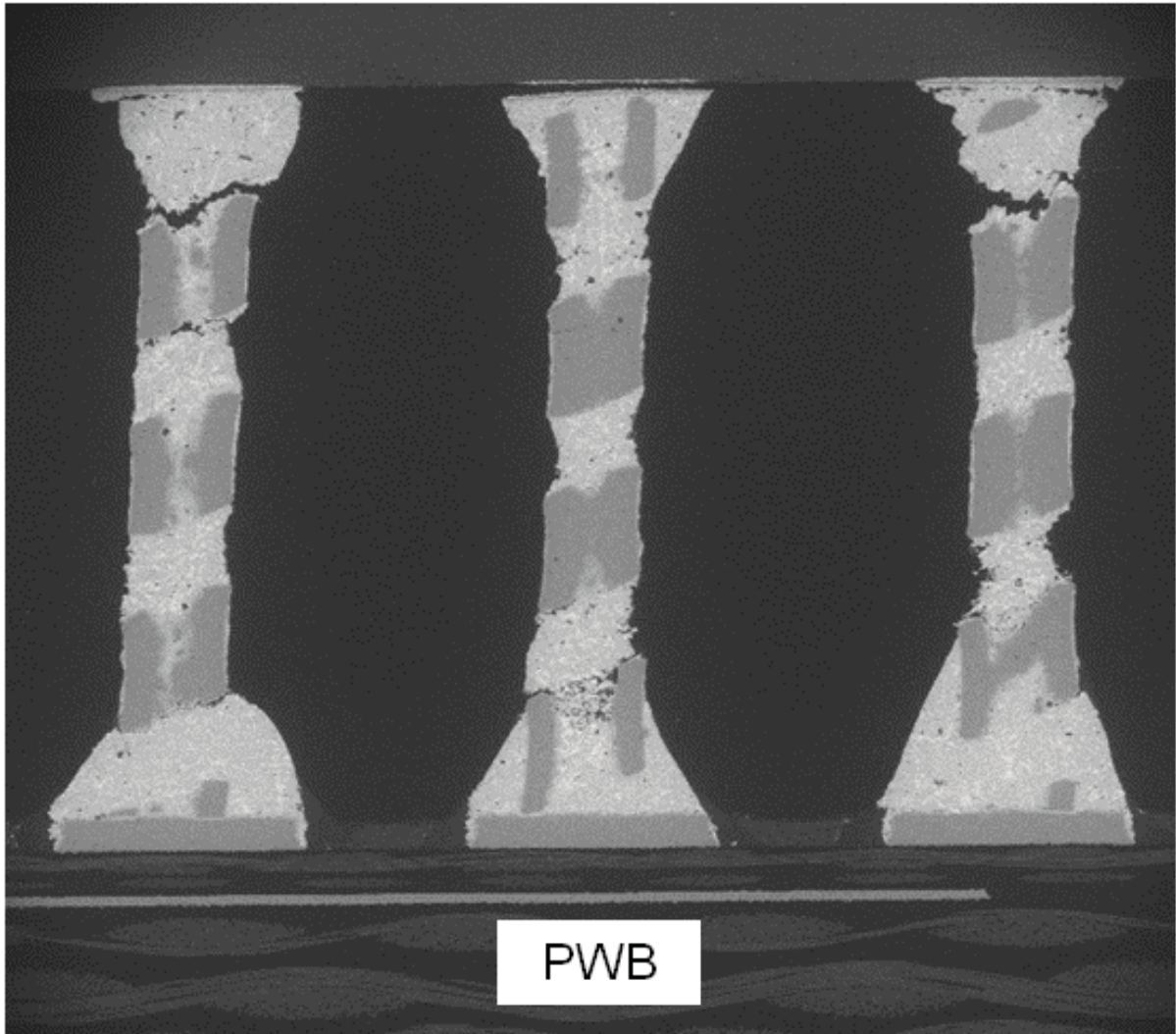


Figure 23. X-section photomicrographs of recolumned/reassembled CCGA 560 I/Os after thermal cycling showing microcracks and separation mostly at the package side (top).

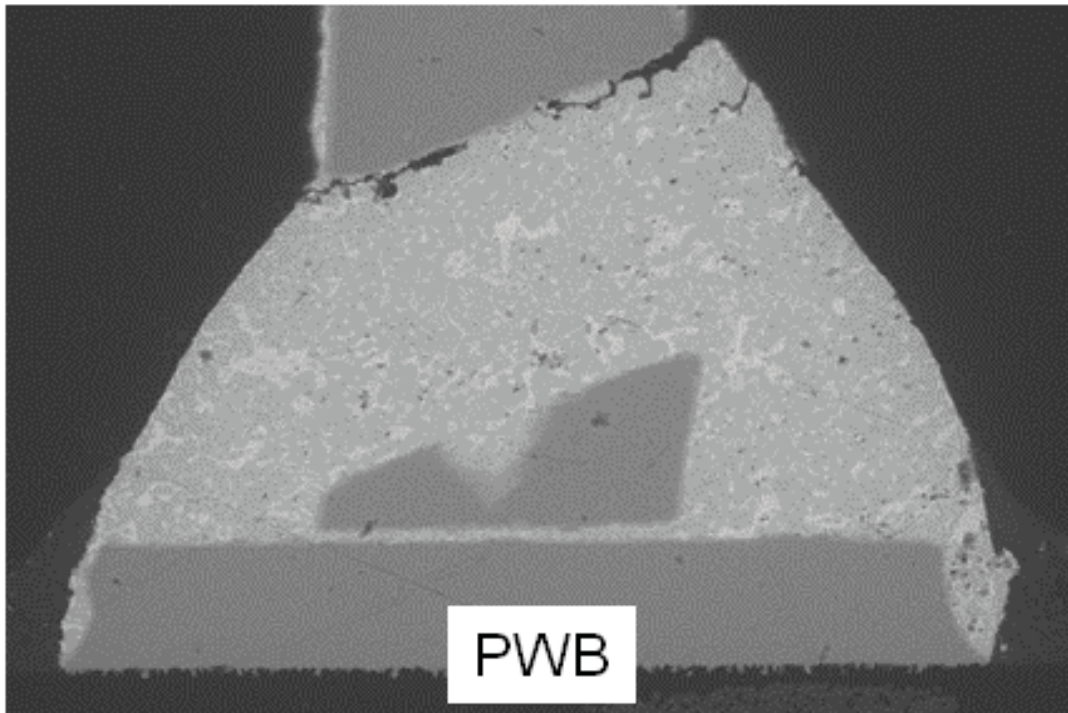
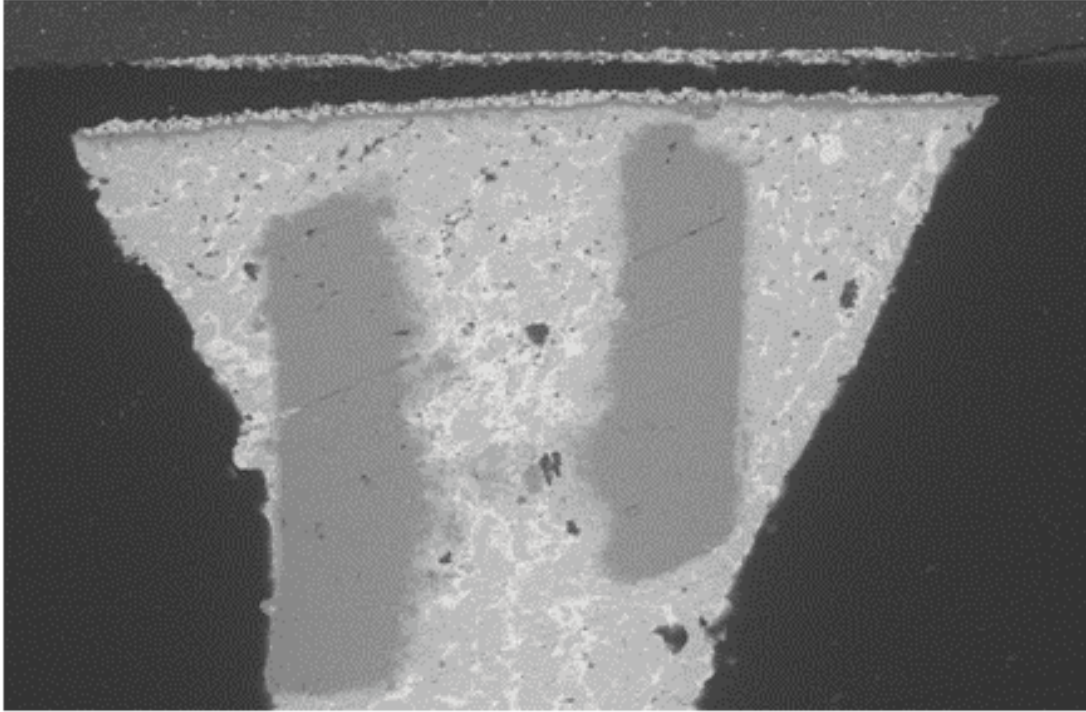


Figure 24. X-section photomicrograph of recolumned/reassembled CCGA 560 I/Os after thermal cycling showing interfacial condition at package and PWB sides. Full cracking at the package side is apparent.

5. Experimental Approaches for High I/O CCGA

5.1 Evaluation of High I/O CCGA

The purpose of this aspect of the investigation was to characterize assembly reliability of a high I/O CCGA package having more than 1,000 recolumn attachments. In contrast to the 560 I/O CCGA, this package had different pad configuration and column type. Differences include:

- Fully populated area array package rather than peripheral array
- Internal flip-chip die rather than wire bond
- 1-mm pitch rather than 1.27-mm
- 35-mm package body rather than 42.5-mm

Similar to other CCGA packages, three columns from each corner were missing; they were intentionally removed by the package supplier in order to improve solder joint reliability. Corner solder columns usually fail first in thermal cycling because they have the longest distances to neutral point (package center).

The original column type in this package is also different from the CCGA 560 I/O; it uses Pb₉₀/Sn₁₀ solder columns with no Cu wrap. Similar to recolumned CCGA 560 I/Os, the Cu wrap columns replaced the virgin columns with high lead composition. Both a typical and a smaller-diameter column were included for evaluation. Smaller-size columns can be used for the high I/O CCGA since the package is smaller and lighter, reducing potential of column breakage due to overloading condition. Because of these significant changes, assembly processing parameters were different from the 560 I/O packages; therefore, they required being tailored again. Tailoring was performed based on previous experiences for similar packages. Additionally, the process was modified on the spot if required, this being possible because only twelve packages were assembled. Ease and consistency in paste deposition, condition of fillet formation after reflow, and solder joint visual appearance were a few important parameters used for tailoring process. Key recolumn and reassembly parameters for processing and evaluation are as follows:

- Successfully recolumned eight high I/O CCGA packages with 20-mil column diameter. No fallout due to recolumning processes.
- Successfully recolumned four CCGA packages with 15-mil column diameter; all solder joint column attachments exhibited acceptable visual quality.
- Prepared two boards for assembly, each having four and two packages with 20- and 15-mil recolumn diameters, respectively
- Utilized two ministencils for solder paste printing, one with 7/23 (thickness/aperture opening) and the other with 8/26 configuration.
- Individually placed each package onto the board using a rework station with optical inspection capability for accurate placement of package on CCGA pattern with paste deposition.

- Assembled ten recolumned, high I/O CCGA packages using a vapor phase reflow machine.
- Individually assembled two recolumned, high I/O CCGA packages using a rework station to establish process steps for assembly and to determine if there are differences between the two techniques in terms of reliability and failures. A rework station is an option for assembly in a low volume manufacturing environment when generally only a few parts assembled. Obviously, it is not an option for high volume manufacturing, but still is used for rework of defected assemblies.

A fully populated board had 6 recolumned high I/O CCGA packages. All assemblies exhibited acceptable—although, in many cases, not ideal—solder joints at the board side, indicated by visual inspection and verified by daisy chain resistance measurement. Inspection of solder joints at the package side is more difficult to perform but, from what was observed, they also appeared to be acceptable. The two test vehicles built under various manufacturing processing conditions were subjected to thermal cycling conditions C only. Details of damage progress was documented by optical microscopy and SEM, and further characterized by cross-sectioning.

5.2 PWB/Package Recolumn

Recolumning was performed using Cu spiral columns at the same facility that CCGA 560 I/Os packages were recolumned. Two recolumn sizes were used, one with 20- and the other with 15-mil diameter. Photomicrographs of the two recolumns at low and high magnifications are compared in Figure 25; the right side shows the 20-mil diameter. Except for the column size differences, solder joints for both conditions have visually acceptable quality with shiny appearance and good fillets. No pull testing was performed; therefore, strength differences between the two column sizes are unknown.

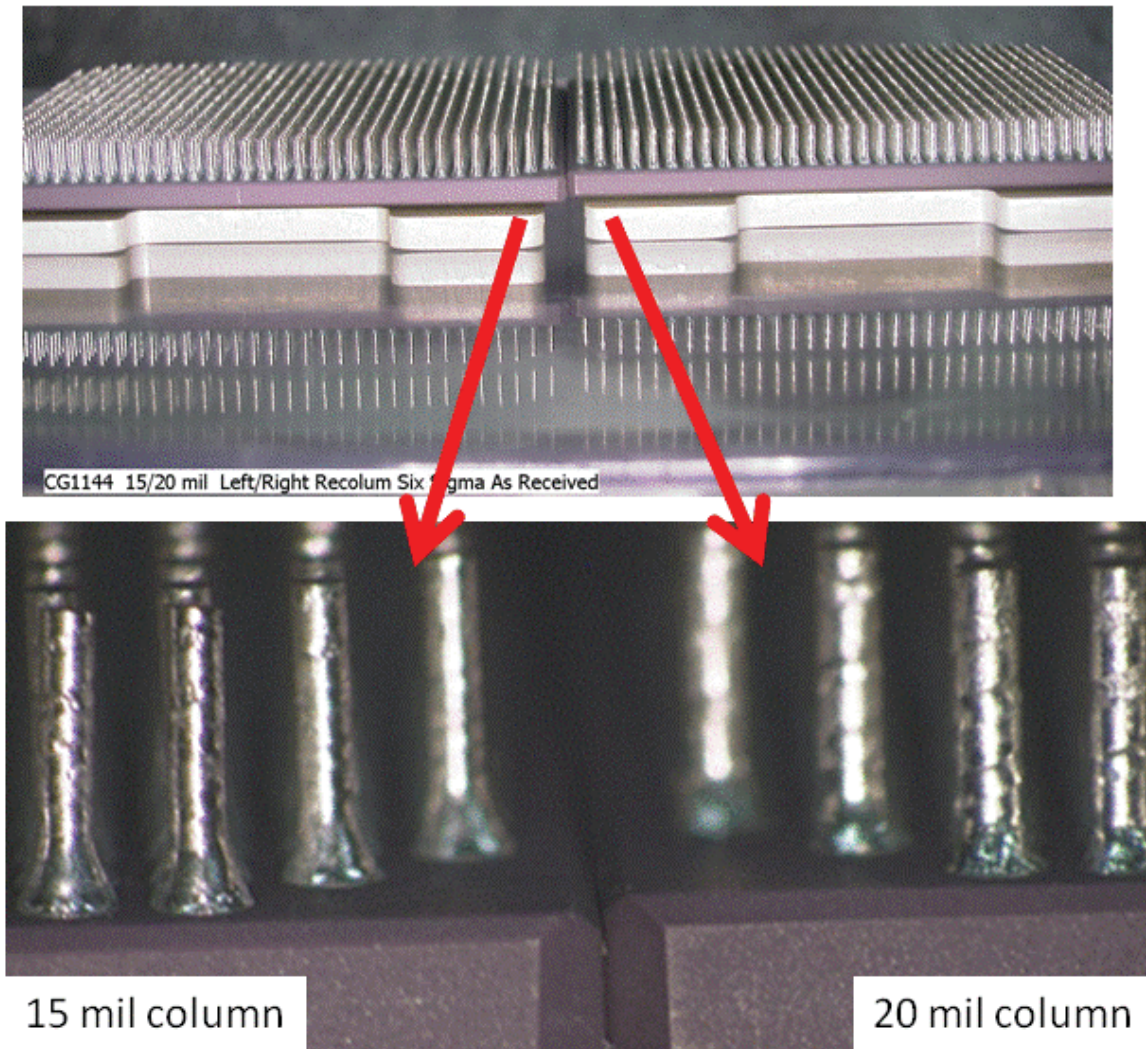


Figure 25. Photomicrographs of the two sizes of recolmned packages (20- and 15-mil columns) at low and high magnifications.

A high temperature, FR-4 PWB with 0.091-inch thickness (as specified by IPC-9701A) with CCGA pads connected to PTHVs was used. Figure 26 depicts an assembled test vehicle having six high I/O packages. Note the input and output traces extending to the board edge and also the probing pads at the package peripheral for manually detecting failures.

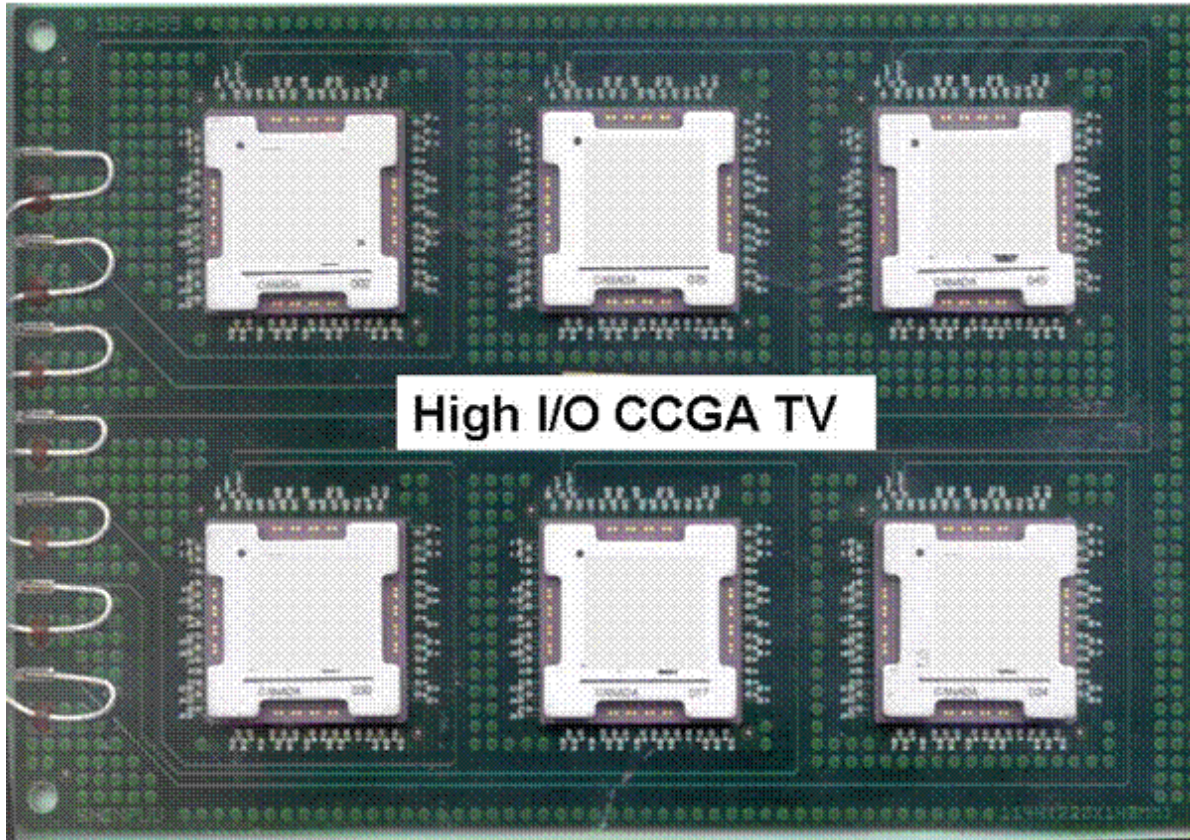


Figure 26. Photograph of an assembled test vehicle having six recolmned, high I/O CCGA packages.

5.3 Stencil Design, Paste Deposition, and Volume Measurement

The stencil thicknesses were 7 and 8 mils, and the two aperture openings were 23 and 26 mils for low and standard volume conditions, respectively. An RMA tin-lead paste was used for paste printing using automatic manufacturing parameters. Figure 27 depicts a photo of a board in which all six CCGA patterns were individually paste printed using a ministencil. After printing, each paste print on the PWB was visually inspected for gross defects such as bridging or insufficient paste. On rare occasion, quality of paste deposition was improved by adding a small amount of paste when insufficient paste was detected. When bridging was discovered, solder paste was removed to open the bridge. In some cases, when the prints had offsets larger than acceptable levels, they were cleaned and reprinted for the second time. Figure 28 depicts optical photomicrographs showing acceptable paste deposition quality (left) and reject quality (right).

Solder paste volumes for selected pads were estimated using a laser profilometer with 3-D dimensional measurement capability. Solder paste areas and heights were measured for solder volume documentation. Measurements were made at numerous locations—including corner and center pads—to gather solder volume data and their corresponding distributions. An example of photomicrographs of paste deposition with 7/23 ministencil (thickness/opening) after paste printing, estimated/calculated solder paste volumes on

each pad, and color-coded paste height distribution measurements are shown in Figure 29. Similar information for the 8/26 ministencil (thickness/opening) is shown in Figure 30.

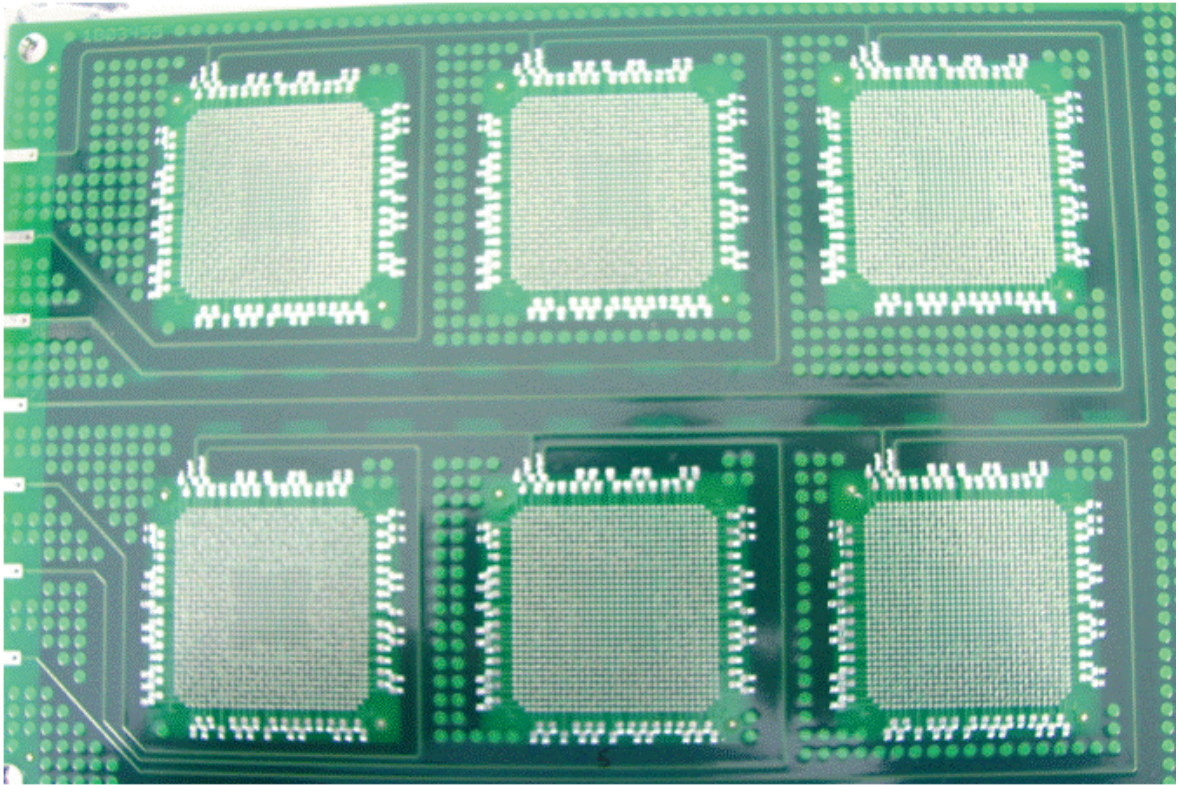


Figure 27. Optical photo of a high I/O CCGA board after paste printing with a ministencil.

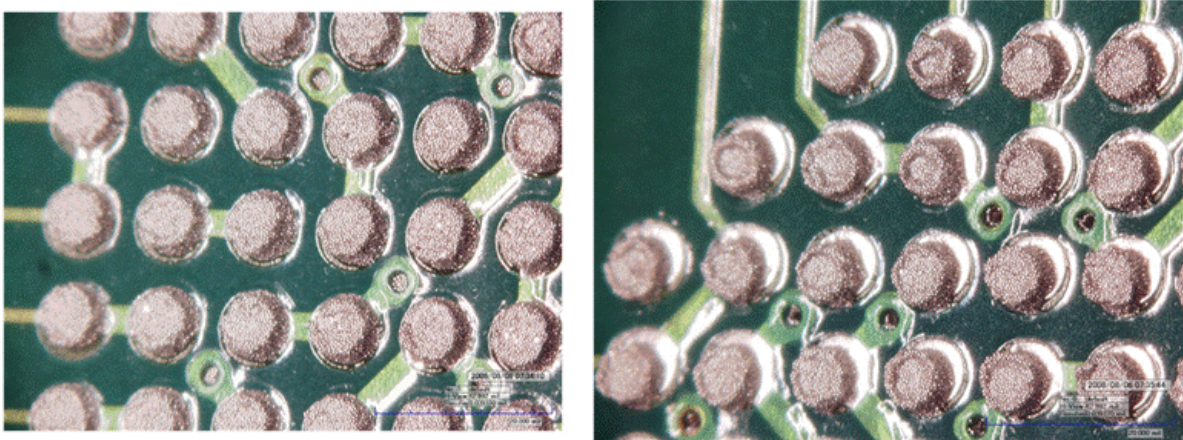


Figure 28. Optical photomicrograph of paste deposition with ministencil with acceptable solder paste quality (left) and reject (right).

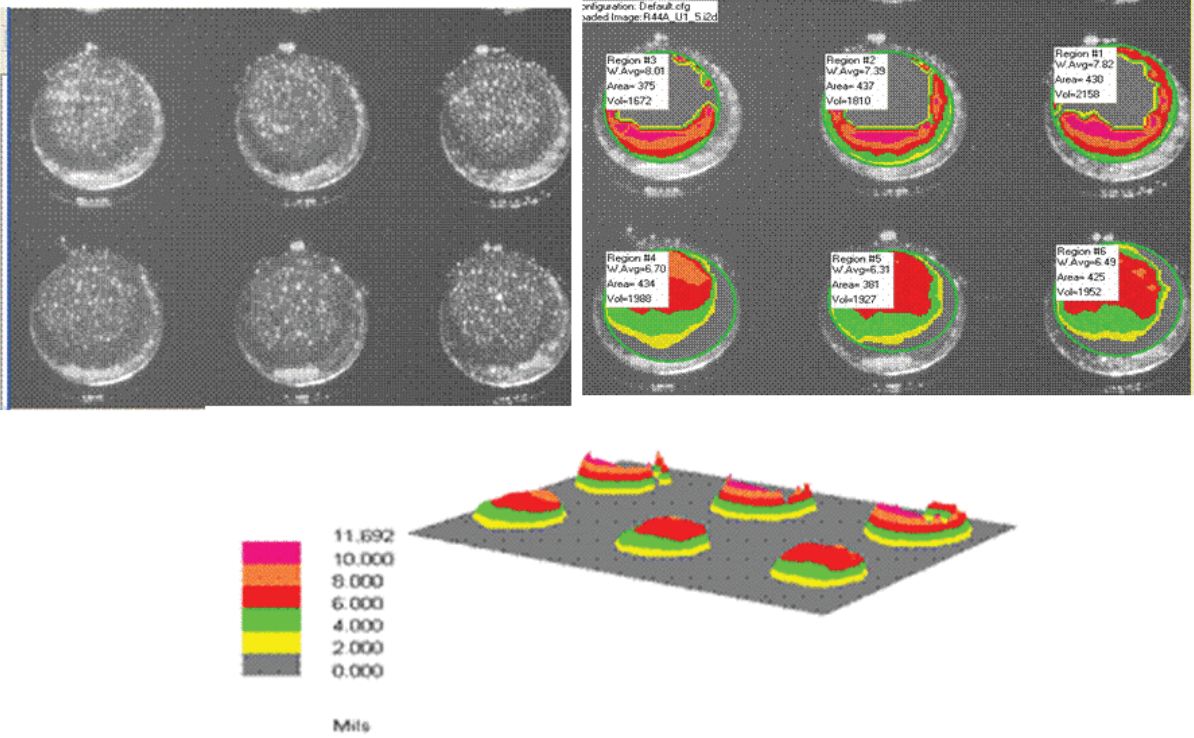


Figure 29. Optical photomicrograph and measured/calculated solder paste information for paste print with ministencil with 7-mil thickness and 23-mil aperture opening diameter.

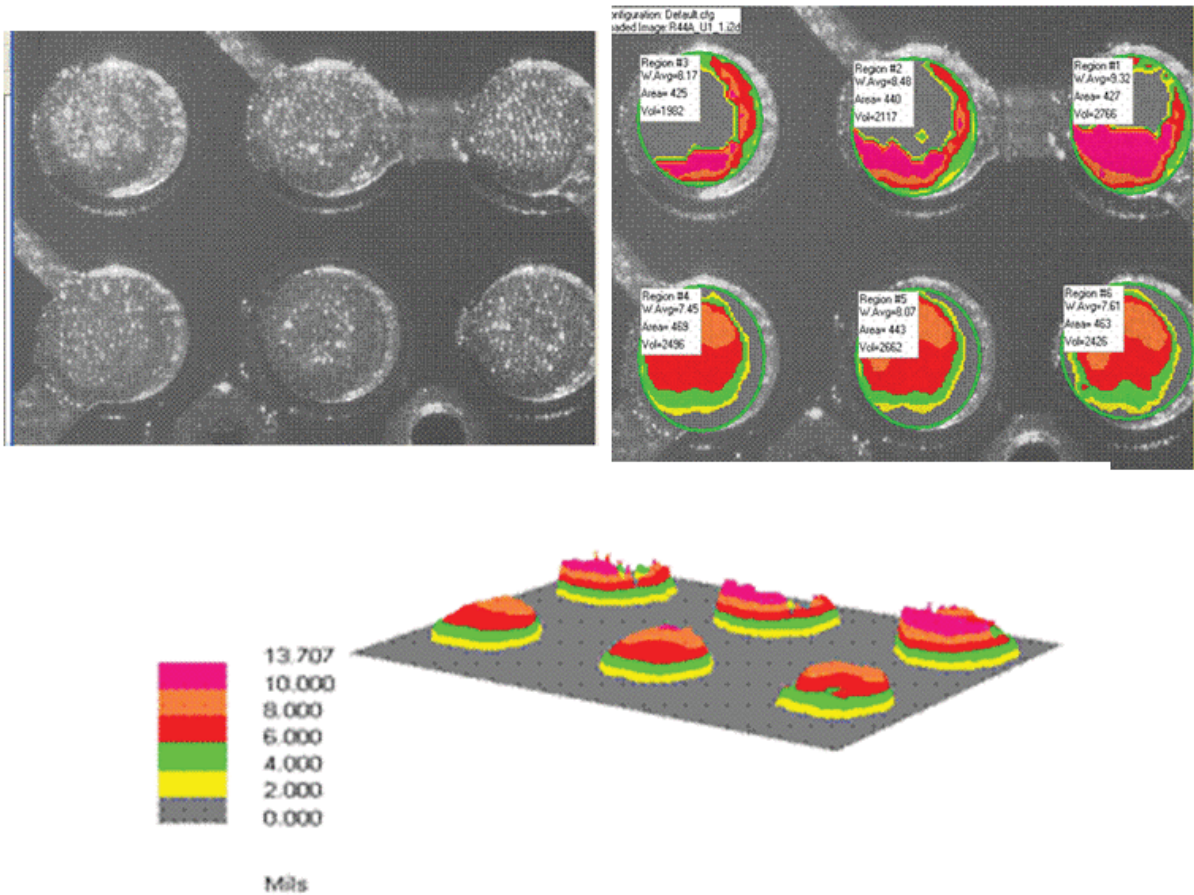


Figure 30. Optical photomicrograph and measured/calculate paste information for paste print with ministencil with 8-mil thickness and 28-mil aperture opening diameter.

5.4 Inspection before Environmental Tests

Visual inspection using an optical microscope was used during assembly to optimize processes based on the visible outer-row column solder conditions. Visual inspection was also performed prior to and during thermal cycling to determine quality of solder joints both at the package and at the board sides. The degree of damage progress in columns and solder joints with cycling was also monitored. Even though only peripheral column interconnections can be inspected, such inspection provides valuable information for CCGA assembly quality and reliability. It provides not only information on solder joint quality, but also on solder damage progress and failure mechanisms since generally CTE mismatch failures first occur in the corner and outer-row columns.

However; for recolumned CCGAs, it was soon recognized that interface close to the package pad are more critical than solder joint quality at the board side. It is more difficult to inspect and document solder joint quality and interface integrity at the package side because the large board area in package vicinity interferes with optical lenses. For this reason, after cycling, boards were cut close to the package body and visually inspected for better identification of damage and cracking even though it is realized that

this was not a representative of inspection for hardware. Optical and SEM photomicrographs were taken before X-sectioning.

Figure 31 depicts representative photomicrographs of solder joint quality at the package and board for a 20-mil recolumned package assembled with low solder volume (7/23). As expected, the solder fillets at the board are minimal for the 20-mil column. The effects of poor fillet conditions on solder joint failures were monitored during thermal cycling, and results were recorded. Note that locations of poor area fillet condition appear to be random rather than preferentially lined up toward a specific direction. For the 15-mil diameter columns, however, solders covered more column surface areas and formed better fillet conditions, as shown in Figure 32. Quality of solder joints at the package side appears to be acceptable for both column sizes.

Figure 33 depicts representative solder joint quality for the 20-mil recolumned package assembled using standard minitencil with 8-mil thickness and 26 aperture opening (8/26). Quality of solder joints for the 20-mil recolumns is improved relative to the lower solder volume condition. Figure 34 depicts quality of solder joints for the 15-mil diameter recolumned package assembly, which appear to be uniform with good fillets. Even for this case, the solder-joint volumes at the package side appear to be excessive and are more than the board side. Reviewing vendor solder attachment process, it was revealed that solder paste deposition volume for recolumn attachment was even higher than the paste volume generated by 8/26 minitencil print condition.

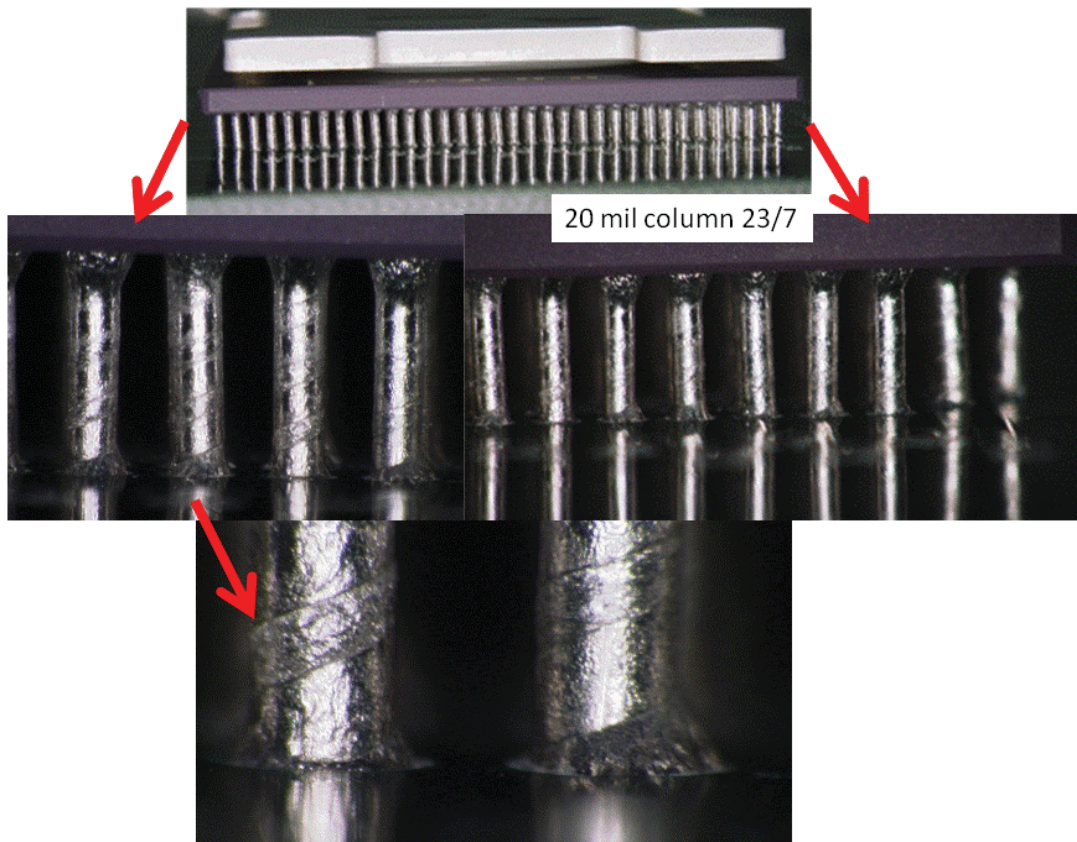


Figure 31. Optical photomicrograph of a 20-mil recolumned package assembled with minitencil having 7-mil thickness and 23-mil aperture opening.

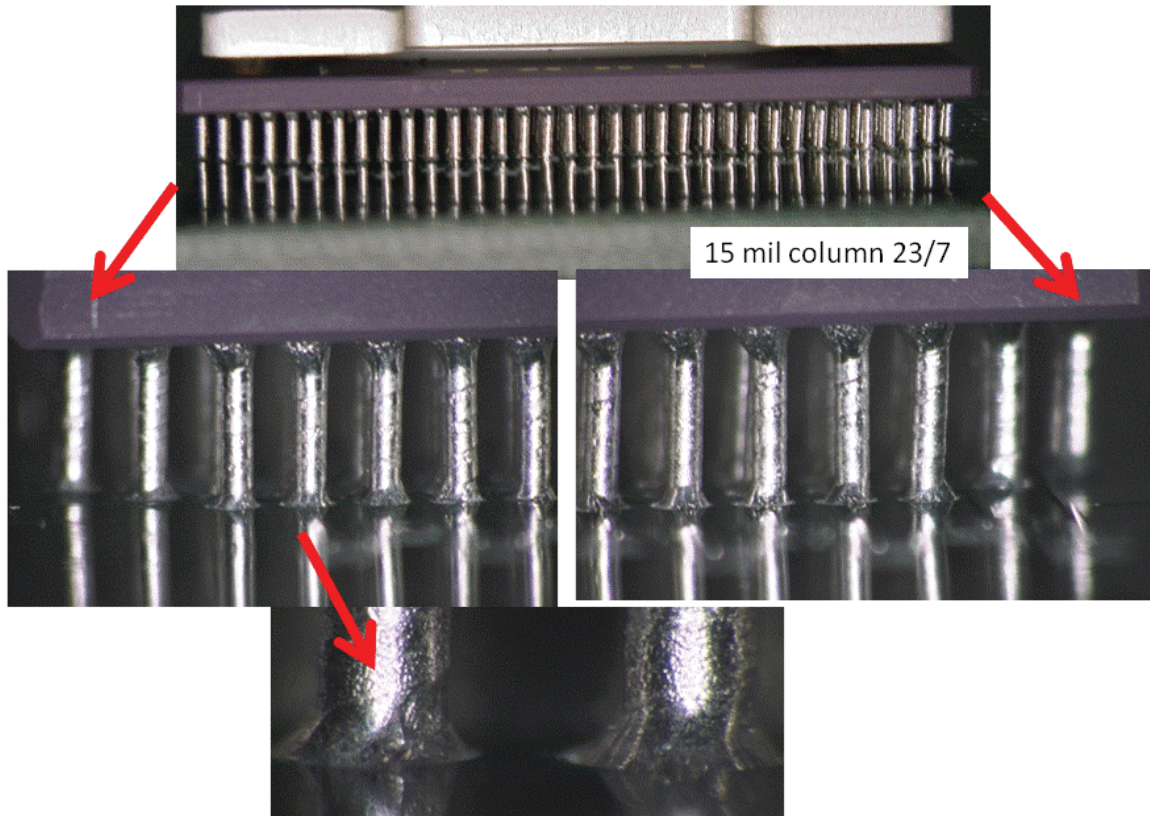


Figure 32. Optical photomicrographs for a 15-mil recolumned package assembled with min-istencil 7/23 (thickness/opening) showing fillet formations.

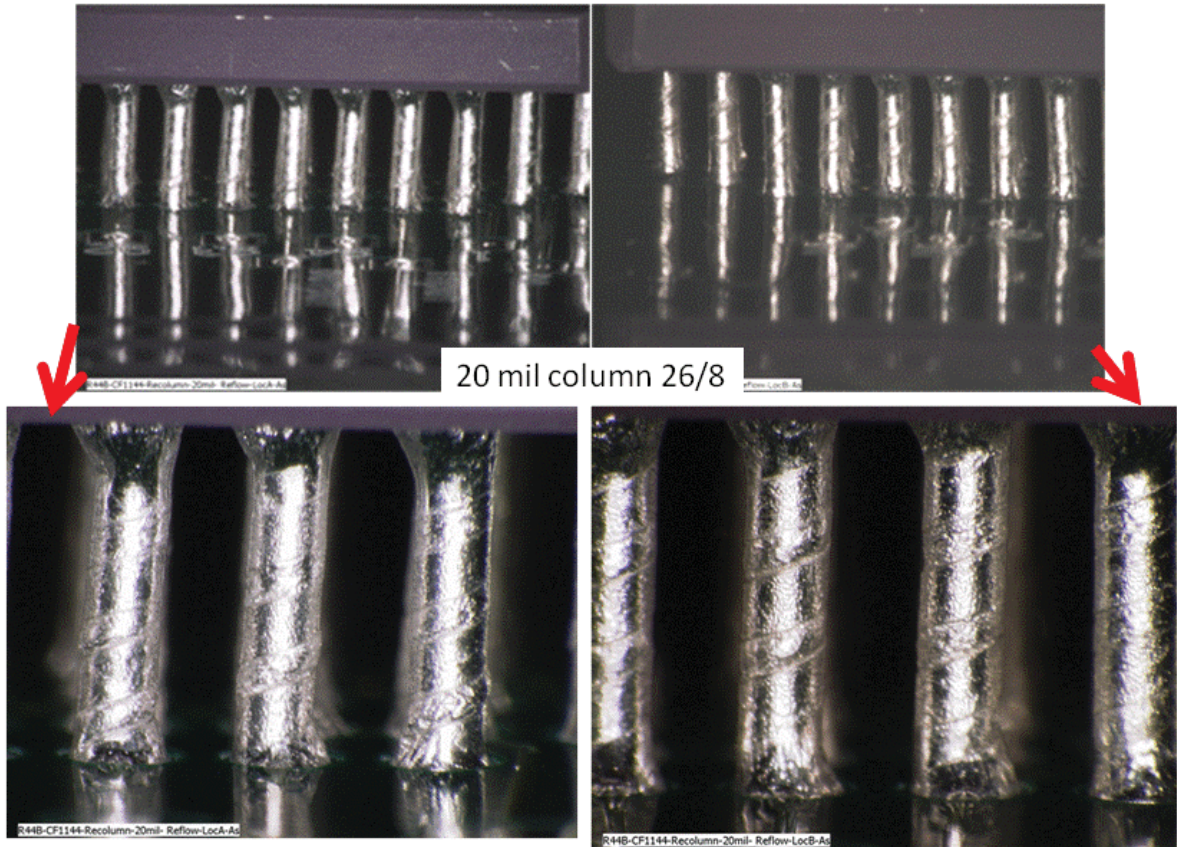


Figure 33. Representative solder joint quality for 20-mil recolumned package assembled using standard ministencil with 8-mil thickness and 26-mil aperture opening (8/26).

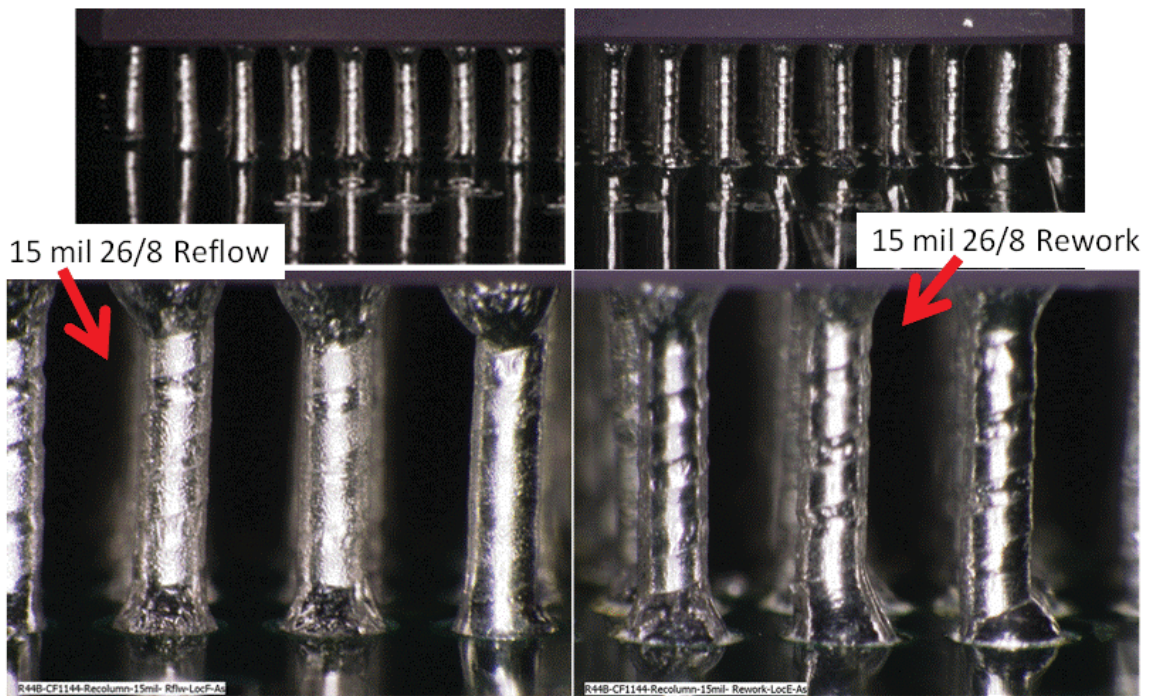


Figure 34. Representative photomicrographs for solder joint with 15-mil recolumned package assembled with 8/26 ministencil (thickness/opening) showing fillet formation.

5.5 Test Results after Thermal Cycling for High I/O Assemblies

5.5.1 Thermal Cycle Condition

From the three thermal profiles, only the Cycle C condition was selected to characterize thermal cycle behavior of the two test vehicles, each having six high I/O CCGA package assemblies. The number of TVs with column and processing variables limited sample size even under one thermal cycle condition. The Cycle C condition ranged from -120° to 85°C with about $5^{\circ}\text{C}/\text{min}$ heating/cooling rate and 10-minute dwells.

5.5.2 Damage Progress Characterizations by Optical Microscopy

Figure 35 depicts a typical optical photomicrograph of a high I/O CCGA assembly after 392 Cycle C thermal cycles ($-120^{\circ}/85^{\circ}\text{C}$). The solder joints at package side exhibit apparent signs of damage, including fine microcracks. Signs of damage are less apparent at the board side even for the lower solder volume condition where in many cases solder joints lack full fillet formation.

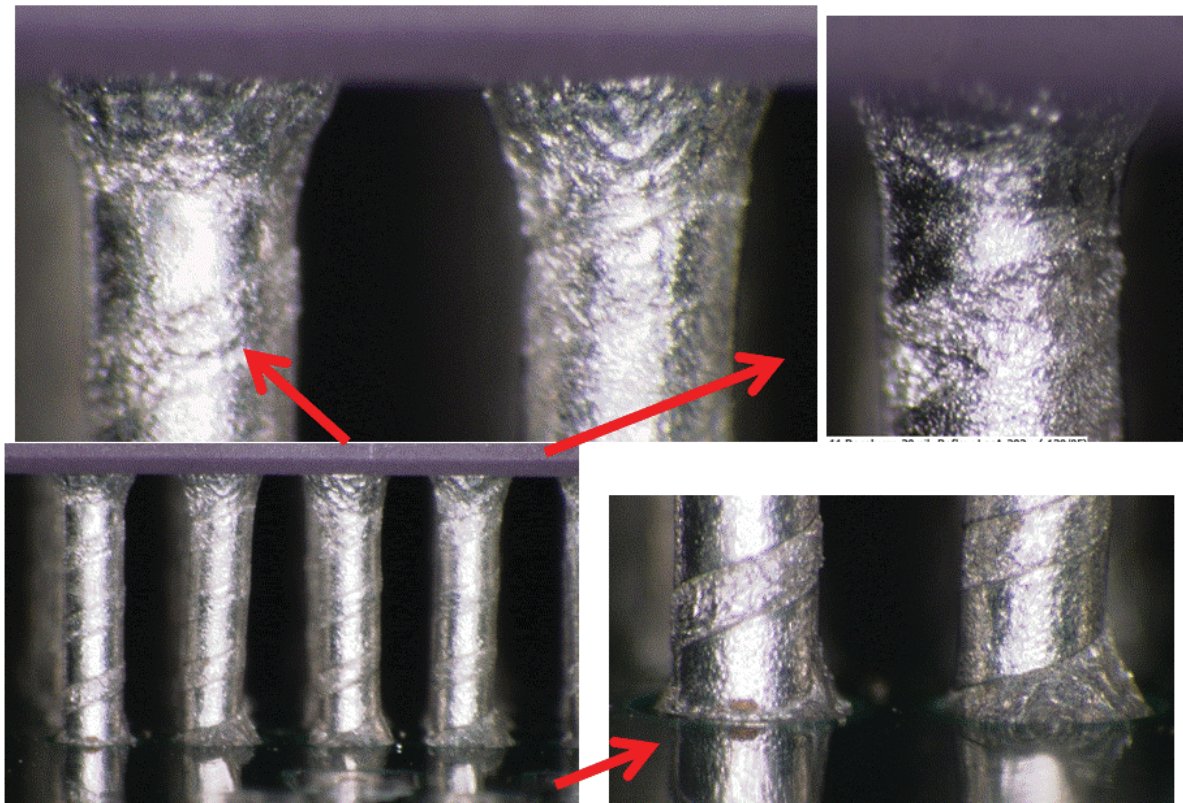


Figure 35. Optical photomicrographs of a 20-mil, recolmned, high I/O CCGA assembly at 392 thermal cycles ($-120^{\circ}/85^{\circ}\text{C}$) with apparent damage/microcracks at package side.

5.5.3 SEM Photomicrographs and X-section

To better characterize microcrack formation of high I/O recolmned package assemblies, two packages were cut close to the package body for optical, SEM, and cross-sectioning. Because of potential failure of recolmns at the package side, it is critical to be able to inspect them; however, it is generally difficult to inspect assemblies at the package side because of board obstruction. Inspection of solder joints at the board side is easier since

solder joints are blocked only by package periphery. For this reason, a thorough optical inspection was performed for two package assemblies after cycling and cutting for X-sectioning. Representative optical photomicrographs of the solder joints at the package side from the cut sample are shown in Figure 36. This figure also includes the pseudo 3-D optical photomicrograph, which is a compilation of images from different optical focus layers. If the optical lenses are aligned correctly with solder joints at the package interface, it is possible to reveal finer microcracks that are generally difficult to detect for a non-cut package assembly.

Photomicrographs clearly depict damage at the package side and even microcracks near the pad interface taken at much higher magnifications. Note that these microcracks could not have been detected during routine optical microscopy evaluation since they are fine and also close to the package interface, making it difficult to detect, as mentioned earlier. Note that these microcracks were first revealed during SEM evaluation at much higher magnifications, and then searched for during an optical inspection.

Figure 37 depicts representative SEM X-ray mapping of columns clearly revealing Cu wrap shown as yellow. Only Cu wrap's edges are apparent through X-ray, possibly because solder surface coating materials were dislocated during thermal cycling, exposing Cu. Cu wrap's edges have a different composition than the tin-lead composition of Cu surface finish and column. Figure 38 depicts representative backscatter SEM photomicrographs showing microstructural features of columns and damage revealed using backscatter under VP/LV chamber condition. Because of compositional contrast, Cu spiral's edges can be seen clearly winding around the columns. Preferential initiation of microcracks at the Cu edges, both near the package and the board sides, is an indication of Cu/column interface weakness, which demonstrates one disadvantage of using Cu spiral. Photomicrographs taken at higher magnifications reveal microcracks surrounding the pads' periphery. The depth of this continuous microcrack cannot be determined by SEM. Destructive x-sectioning reveals depth and failure mechanisms.

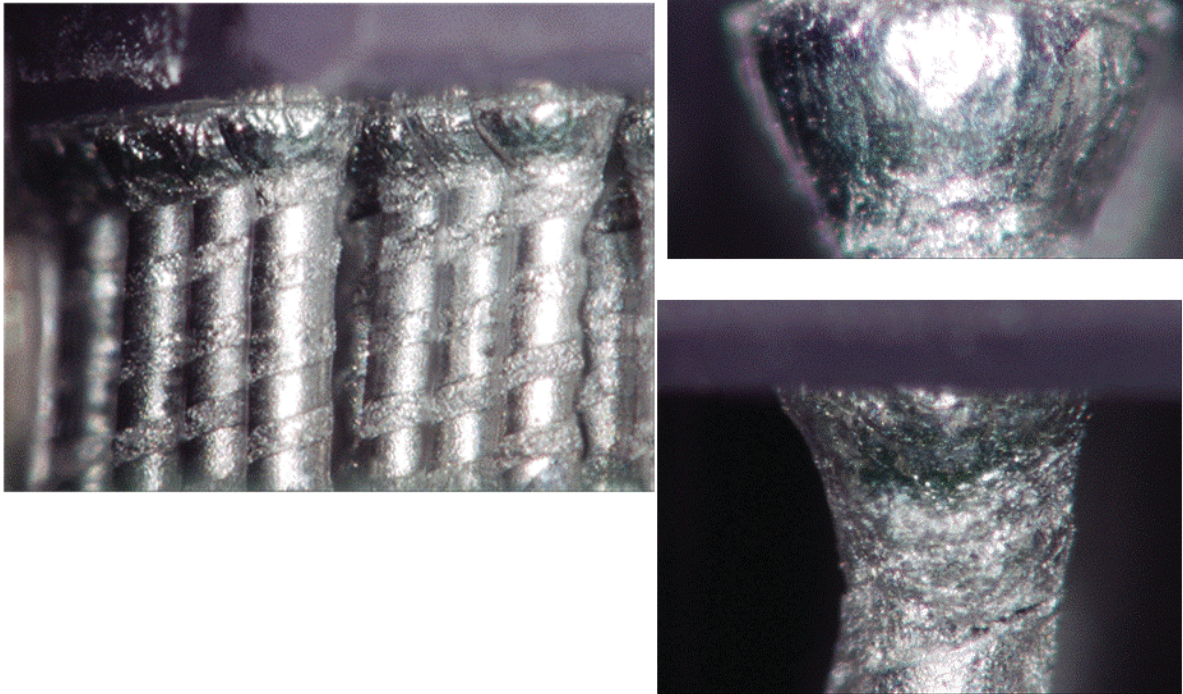


Figure 36. Representative optical photomicrographs, including those with pseudo 3-D optical photomicrograph, showing damage and microcracks at the package side.

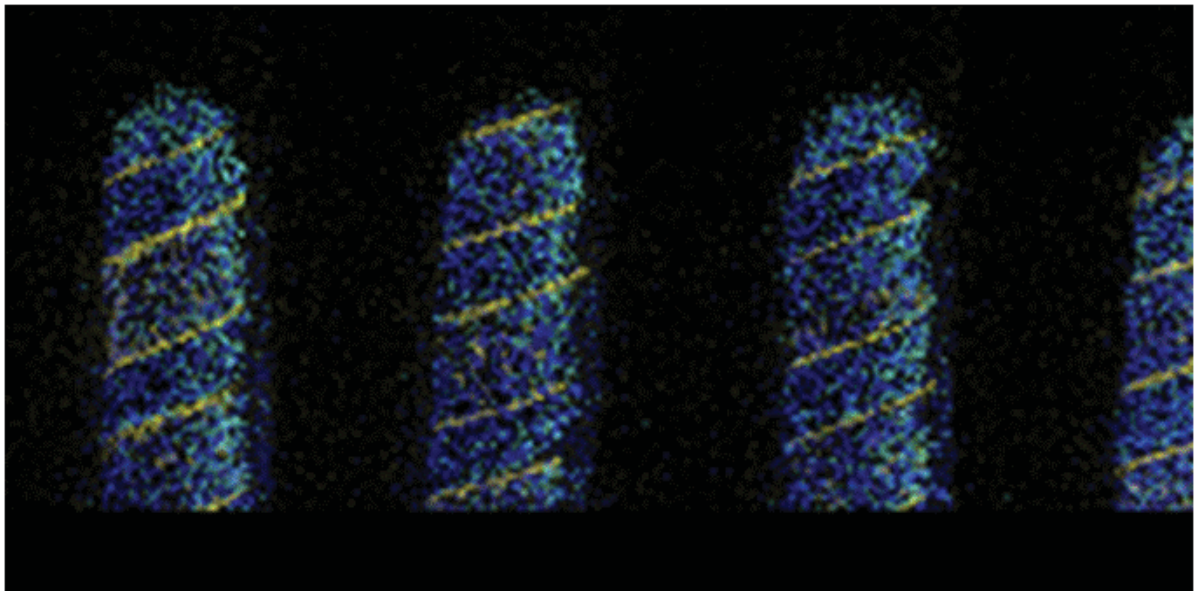


Figure 37. Representative X-ray mapping of columns clearly reveals Cu spiral/wrap as yellow with background tin-lead solder column.

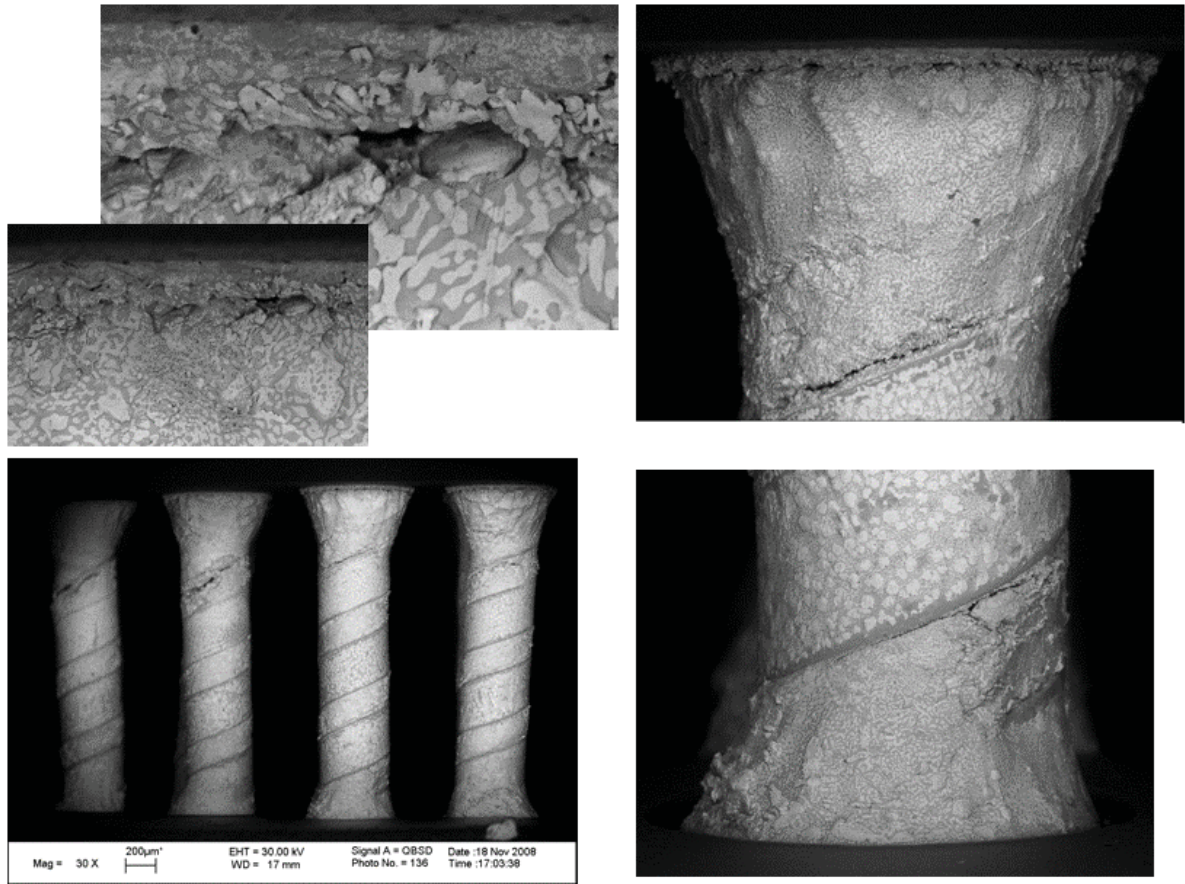


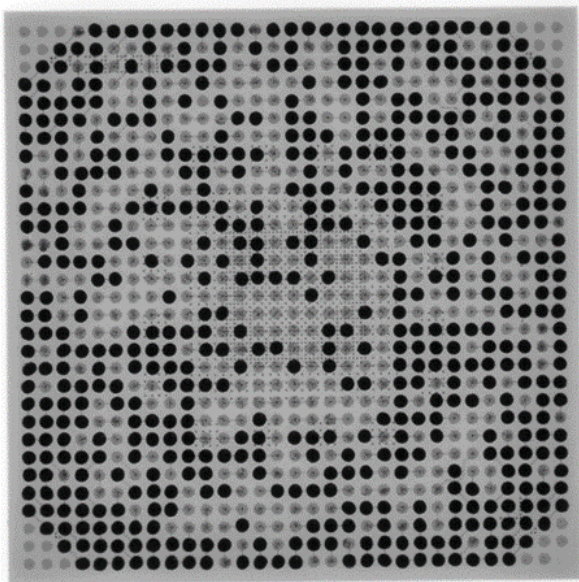
Figure 38. SEM photomicrographs of assemblies prior to cross-sectioning showing damage level and microcracks.

5.6 Failure Behavior of a High I/O CBGA

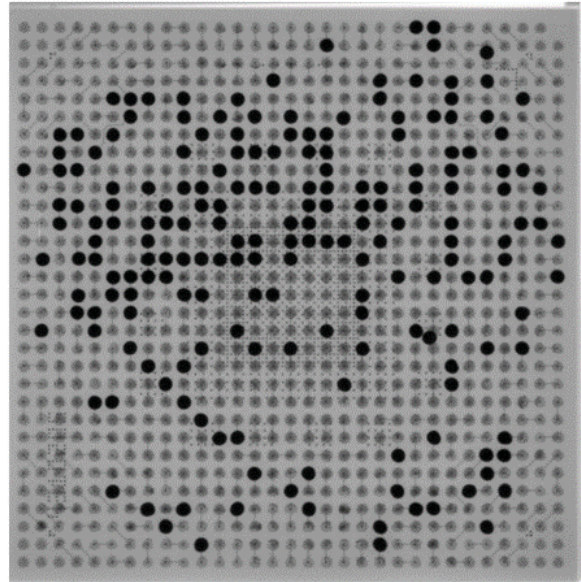
Failure behavior of a high I/O CBGA was determined by a paper jointly published in collaboration with Celestica, Inc., covering a literature survey [22]; some of the results for the RIA3 TV [23], [24]; and additional thermal cycle test results gathered at both facilities. One of the package assemblies was CBGA with 927 I/Os. Failure data for this assembly were presented previously, showing early failure compared to PBGA package assemblies. The RIA3 TVs were also subjected to three thermal cycles at JPL. Results confirm early failures of these assemblies, which are much lower than those reported in this report for recolumned CCGA package assemblies. The CBGA packages could be easily removed from the board after a number of cycles. The failed packages that had balls on them at various locations were subjected to a 2-D X-ray characterization.

A real time, 2-D X-ray system with a stationary microfocus source intensity and off-axis rotational capability was used to determine distribution of solder joint failures from either package or board sides. Figure 39 depicts X-rays of high I/O CBGA failed packages from the two different thermal cycle conditions. Dark circular spots on the X-ray photomicrographs represent balls that remained on the package; i.e., solder joint failures

from the board side. Failure distributions are significantly different from one type cycle profile to another.



-55/125C



-120/85C

Figure 39. X-rays photographs of failed high I/O CBGA assemblies showing failure mechanism changes possibly due to thermal cycle profiles.

6. Conclusions

The conclusions based on the status of thermal cycling studies for the three CCGA package assemblies are as follows:

- The literature survey identified trends in area array packages that:
 - High I/O packages are being transitioned from ball grid arrays to column grid array for high reliability applications;
 - Within the package, wire-bond limits the package I/O and a flip chip is required for higher I/O packages;
 - The hermetic package switches to non-hermetic to accommodate flip-chip die;
 - Pb-Sn columns is being replaced with the Cu spiral columns to increase stiffness; and
 - Pb-Sn solders are being replaced with Pb-free solder alloys to meet lead-free conversion by industry.
- The literature survey revealed that, in most cases, resistance in thermal cycle reliability for high I/O CCGA packages with flip-chip die and 1-mm pitch decreased compared to the lower I/O package with wire bond and pitch of 1.27 mm.
- The survey revealed the contrast of the effect of solder volume on thermal cycles to failures between CBGA and CCGA assemblies. For CBGAs, cycles to failure (CTFs) increased with solder volume to some level since increases in solder volume causes increases in the solder ball standoff approaching column configuration.
- The Cu spiral recolumn version of the CCGA 560 I/O package without its original ceramic layer interposer exhibited good attachment interconnection strength after recolumning and when exposed to isothermal aging at 125°C to 500 hours.
- Average pull strength of recolumned interconnections decreased by about 20% after 500 hours of aging at 125°C. Strength reduced from 1585 to 1270 grams after 500 hours aging and decreased from 1598 to 1294 grams for those that had one additional reflow exposure prior to aging.
- In a previous investigation, thermal cycle reliability and failure mechanisms for CCGA 560 I/O with interposer were investigated. Failures were from either the package (between interposer and package) or the board side.
- Numerous manufacturing variables were evaluated for reassembly of recolumned CCGA 560 I/Os. Only limited assemblies exhibited visually acceptable solder joint quality and daisy chain continuity with low resistance values. Variables evaluated included solder paste deposition volume, assembly on a smaller pad designed for its PBGA counterpart, and reflow of solder paste alloys using either vapor phase reflow machine or rework station.
- Based on only a few test samples subjected to thermal cycling and visual inspection, it appears that recolumned 560 I/O package with no interposer is a viable rework so-

lution from an assembly perspective only. Further work is required to substantiate these test results.

- A high I/O (>1000 I/Os) CCGA package was successfully recolumned using either 20- or 15-mil column diameters.
- The recolumned, high I/O CCGAs were successfully assembled using ministencils providing low and medium solder volumes, and they were reflowed using either vapor phase reflow machine or rework station.
- All high I/O CCGA assemblies passed 200 severe thermal cycles with no apparent visual damage or daisy chain failures. However, damage and fine microcracks were apparent at higher cycles. Representative optical and SEM photomicrographs at higher magnifications with microstructural resolution showing microcracks at the package side were presented.
- Based on limited thermal cycle test results and visual inspection during thermal cycling, recolumning of the high I/O CCGAs is a viable option from a solder attachment perspective only.
- Assemblies of a high I/O CBGA exhibited significantly lower cycles to failure; therefore, high I/O CBGAs are not recommended for high reliability applications.

7. NASA Applications

Laboratory tests and the literature survey yielded the following conclusions pertaining to the use of high I/O CCGA package assemblies for NASA electronic systems:

- Qualification guidelines and quality assurance indicators were established and presented for high I/O CCGA packages based on tensile test data for recolunmed CCGA packages, process controls for paste deposition and assembly using vapor phase or rework station, thermal cycle test data, and monitoring damage progress and characterization using X-ray, optical, SEM, and cross-sectioning.
- It was revealed that extremely limited flight heritage exists for ceramic area array packages; therefore, package qualification is required for a specific application using lessons learned guidelines and quality assurance indicators presented in this investigation.
- Thermal cycle test data indicates that CCGA 560 I/O packages with ceramic interposer can have acceptance performance only in a relatively benign and controlled environment.
- The high I/O CCGA assemblies, including the one evaluated here with no interposer but smaller package size, exhibited better thermal cycling resistance than larger CCGA 560 I/Os with interposer.
- Even though CCGAs are COTS packages, their high reliability package versions go through a more stringent screening with added cost and long-time delay in delivery schedule. Understanding key issues in package recolumning and reassembly are critical from both schedule and cost perspectives.
- This investigation clearly revealed that recolumning of CCGA packages using Cu spiral column is feasible. Assembly process may be challenging for larger packages and optimization required. The effects of rework, recolumn, and reassembly on functional die are unknown since dummy daisy chain chips were used in this evaluation.
- High I/O CCGA packages with smaller package sizes can be recolumned and reassembled with some decrease, potentially, in long-term thermal cycling resistance. Even though the effect of rework on die is unknown, this investigation demonstrated feasibility of recolumning and reassembly for CCGA packages.

For NASA missions with relatively benign environments, most CCGA package assemblies have adequate thermal cycle resistance. For longer NASA missions, CCGA packages characterized in this investigation with relatively smaller package dimensions and higher I/Os to about 1,000 (with either virgin or recolumn attachment) may have adequate thermal cycle reliability resistance. PQV shall be performed to validate and tailor requirements for a specific application.

8. Acronyms and Abbreviations

AAP	Area Array Package
BGA	Ball Grid Array
BoK	Body of Knowledge
CBGA	Ceramic Ball Grid Array
CCGA	Ceramic Column Grid Array
CGA	Column Grid Array
COTS	Commercial, off-the-shelf
CQFP	Ceramic Quad Flat Pack
CSP	Chip Scale (Size) Package
CTE	Coefficient of Thermal Expansion
CTF	Cycles to Failure
Cu	Copper
DOE	Design of Experiments
EDX	Energy Dispersive X-ray
EMS	Electronics Manufacturing Service
ENIG	Electroless Nickel Immersion Gold
FCBGA	Flip-Chip Ball Grid Array
FPBGA	Fine Pitch BGA, a.k.a. Chip Scale Package (CSP)
HASL	Hot-Air Solder Leveling
I/O	Input/Output
IPC	Association Connecting Electronics Industries
KGD	Known Good Die
LGA	Land Grid Array
NEPP	NASA Electronic Parts and Packaging
Ni	Nickel
NSMD	Non-Solder Mask Defined
OSP	Organic Solderability Preservative
Pb	Lead
PBGA	Plastic Ball Grid Array
PCB	Printed Circuit Board
PQV	Package Qualification and Verification
PTH	Plated-through Hole
PTHV	PTH Via
PWA	Printed Wiring Assembly

PWB	Printed Wiring Board
QA	Quality Assurance
QFP	Quad Flat Pack
RMA	Rosin Mildly Activated
RT	Room Temperature
SAM	Scanning Acoustic Microscopy
SEM	Scanning Electron Microscopy
SMC	Surface Mount Components
SMD	Solder Mask Defined
SMT	Surface Mount Technology
Sn	Tin
TC	Thermal Cycle
TCE	Also CTE, Thermal Coefficient of Expansion
Tg	Glass Transition Temperature
TMA	Thermal Mechanical Analysis
TSOP	Thin Small Outline Package
TV	Test Vehicle
XRF	X-ray Florescence

9. Acknowledgements

The author would like to acknowledge many people from industry and JPL who were critical to the progress of this activity. The author extends his appreciation to program managers of the NASA Electronic Parts and Packaging Program (NEPP), including Michael Sampson, Ken Label, Charles Barnes, and Phillip Zulueta, for their continuous support and encouragement.

10. References

- [1] Ghaffarian, R., “Thermal Cycle Reliability and Failure Mechanisms of CCGA and PBGA Assemblies With and Without Corner Staking,” *IEEE Transactions on Components and Packaging Technologies*, Vol 31, Issue 2, June 2008, Pages 285–296.
- [2] Ghaffarian, R., “CCGA Packages for Space Applications,” *Microelectronics and Reliability*, Volume 46, Issue 12, December 2006, Pages 2006–2004.
- [3] Ghaffarian, R., “Area Array Technology for High Reliability Applications,” Chapter 16 in *Micro-and Opto-Electronic Materials and Structures: Physics, Mechanics, Design, Reliability, Packaging*, ed. E. Suhir, Editor (Springer, 2006).
- [4] Ghaffarian, R., “Shock and Thermal Cycling Synergism Effects on Reliability of CBGA Assemblies,” *2000 IEEE Aerospace Conference Proceedings* (2000), p. 327.
- [5] Ghaffarian, R., “Characterization and Failure Analyses of Lead-Free Solder Defects,” Chapter 10 in *Lead-Free Solder Interconnect Reliability Book*, ed. D. Shangquan (ASM International, 2005).
- [6] Ghaffarian, R., “BGA Assembly Reliability,” Chapter 20 in *Area Array Packaging Handbook*, ed. K. Gilleo (McGraw-Hill, 2004).
- [7] Fjelstad, J., Ghaffarian, R., Kim, Y. G., *Chip Scale Packaging for Modern Electronics* (Electrochemical Publications, 2002).
- [8] Ghaffarian, R., “Chip Scale Package Assembly Reliability,” Chapter 23 in *Area Array Interconnect Book*, eds. K. Puttlitz, and P. Totta (Kluwer Academic Publishers, 2002).
- [9] Ghaffarian, R., Kim, N.P., “Reliability and Failure Analyses of Thermally Cycled Ball Grid Array Assemblies,” *IEEE Transactions on Components and Packaging Technologies*, Sept 2000, Pages 528–534.
- [10] White Paper, “Solder Column Qualification for Ceramic Column Grid Array (CCGA),” Aeroflex Colorado Springs, July 2008: <http://ams.aeroflex.com/ProductFiles/AppNotes/AeroflexCCGAQualWhitePaper.pdf>
- [11] Kuang, R., Zhao, L., “Thermal Cycling Test Report for Ceramic Column Grid Array Packages (CCGA),” Actel Corp.: http://www.actel.com/documents/CCGA_board_level_testing_report.pdf
- [12] Master, R.N. and Ong, O.T., “Ceramic Grid Array Technologies for ACPI Applications” *The Proceedings of Surface Mount International*, Chicago, IL (Sept. 25–28, 2000).
- [13] Device Reliability Report, second quarter 2008, Xilinx Corp.: http://www.xilinx.com/support/documentation/user_guides/ug116.pdf
- [14] Farooq, M., Goldmann, L., Martin, G., Goldsmith, C., Bergeron, C., “Thermo-Mechanical Fatigue Reliability of Pb-Free Ceramic Ball Grid Arrays: Experimental Data and Lifetime Prediction Mounting,” *The Proceeding of IEEE Electronic Components and Technology* (2003), pp. 827–833.

- [15] Interrante, M. et al., “Lead-Free Package Interconnection for Ceramic Grid Arrays,” *IEEE/CPMT/SEMI Int’s Electronics Manufacturing Technology Symposium* (2003).
- [16] CBGA Assembly and Rework, IBM User’s Guideline (May 23, 2002).
- [17] Column Grid Array and Rework, IBM User’s Guideline (July 22, 2002).
- [18] NASA-STD-8739.3, Soldered Electrical Connections.
- [19] NASA-STD-8739.2, Workmanship Standards for Surface Mount Technology.
- [20] IPC-7711, “Rework, Modification and Repair of Electronic Assemblies,” IPC, Association Connecting Electronics Industries.
- [21] IPC-9701A, “Performance Test Methods and Qualification Requirements for Surface Mount Solder Attachments,” <http://www.feinfocus.de/>
- [22] Ghaffarian, S. Bagheri, H. McCormick, I. Sterian, “Reliability of Lead-Free and Tin-Lead Solders for PBGA Assemblies,” IMAPs RF Packaging Workshop, San Diego, Sep 16–18, 2008.
- [23] McCormick, H., et al, “Mixing Metallurgy: Reliability of SAC Balled Area Array Packages Assembled Using SnPb Soldering,” SMTA International, Sept 2006.
- [24] Snugovovsky, P., et al., “Failure Mechanisms of SAC305 and SAC405 in Harsh Environment and Influence of Board Defects Including Black Pad,” SMTA International, Sept. 2006.

11. Vendor Report on Column Attachment Strengths

Column Pull Test of JPL Column Grid Arrays

Document #: FAR-SS-2-080229

ABSTRACT

Minerva M. Cruz
Minerva M. Cruz
Failure Analysis Engineer

1.0 Background

Two column grid array specimens, with 22-mil diameter columns, were processed using typical Six Sigma column attach process. Pull test was then performed after column attach and after aging the specimens for 100, 247, and 500 hrs at an aging temperature of 125°C. Details of the study are discussed below.

2.0 Objective

The objectives of this study are:

- (a) to determine the column pull strength of the columns after column attach and after aging
- (b) to determine the effect of aging on the strength of the column
- (c) to determine the nature of the column pull strength as a function of aging time

3.0 Experimental Procedure

Two column grid array specimens, named Specimen #300 and Specimen #400 were processed using typical Six Sigma column attach process. After column attach, Specimen #400 was reflowed one more time to simulate board mounting process. After column attach, 15 columns were randomly selected and then pulled from each specimen. To determine the effect of aging on the strength of the columns, the specimens were aged isothermally for 100, 247, and 500 hours at 125°C. After each aging time, 15 columns were randomly selected and then pulled from each specimen. The average values for each aging time for each specimen were then obtained and plotted as a function of aging time.

4.0 Results and Discussion

Shown in Table 1 are the average pull test values for Specimen #300 for each aging time. The raw data are tabulated in Appendix A. Only one failure mode was found in all the pulled columns, namely, column failure, as shown in Figure 1.

Table 1. Average and standard deviation values of pull forces as a function of aging time for Specimen #300.

Aging Time (hours)	Average Pull Force (grams)	Standard Deviation (grams)
0	1585	70
100	1383	56
247	1316	62
500	1270	49



Figure 1. An image of a typical column failure mode found in Specimen #300.

The plot of the averages of the pull forces as a function of aging time, for Specimen #300 is shown in Figure 2. As can be seen from the graph, there was a decrease in the average pull force after 100 hrs of aging. The average pull force remained constant after that. Student t-test calculations (assuming equal means), at a confidence level of 95%, indicated an statistical differences between no aging and 100 hrs of aging. The force remains the same after that. Student t-test calculations are tabulated in Appendix B. Overall, the mean pull force decreased by 20% over the 500- hours of aging.

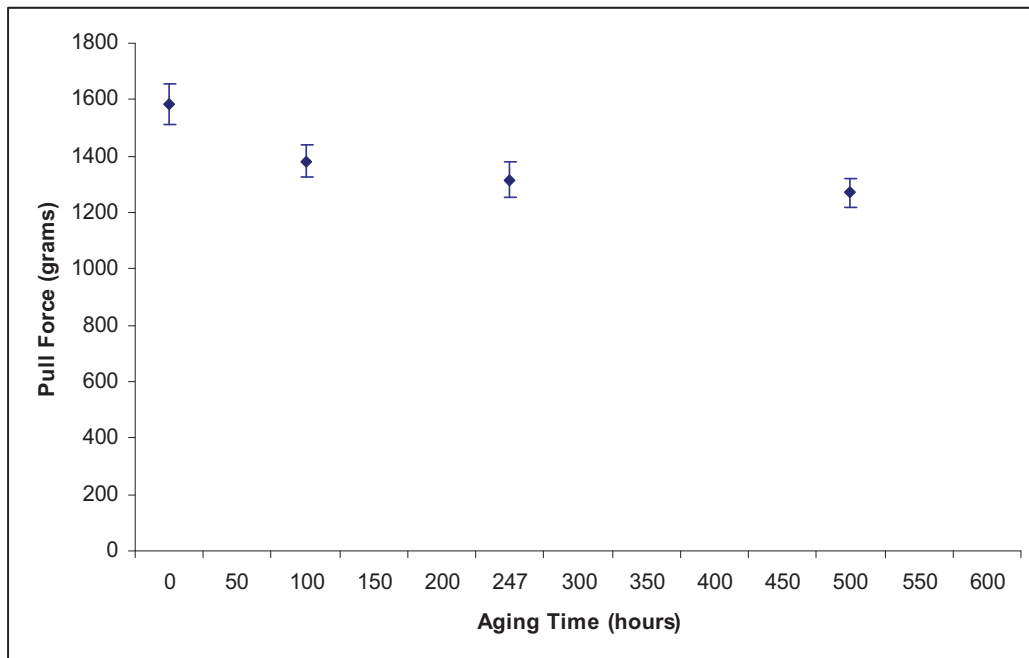


Figure 2. Pull force as a function of aging time, for Specimen #300.

The average pull force for each aging time for Specimen #400 is shown in Table 2, and the raw data are tabulated in Appendix A. A typical column breakage failure mode is shown in Figure 3.

Table 2. Average and standard deviation values of pull forces as a function of aging time for Specimen #400.

Aging Time (hours)	Average Pull Force (grams)	Standard Deviation (grams)
0	1598	80
100	1338	57
247	1273	64
500	1294	41

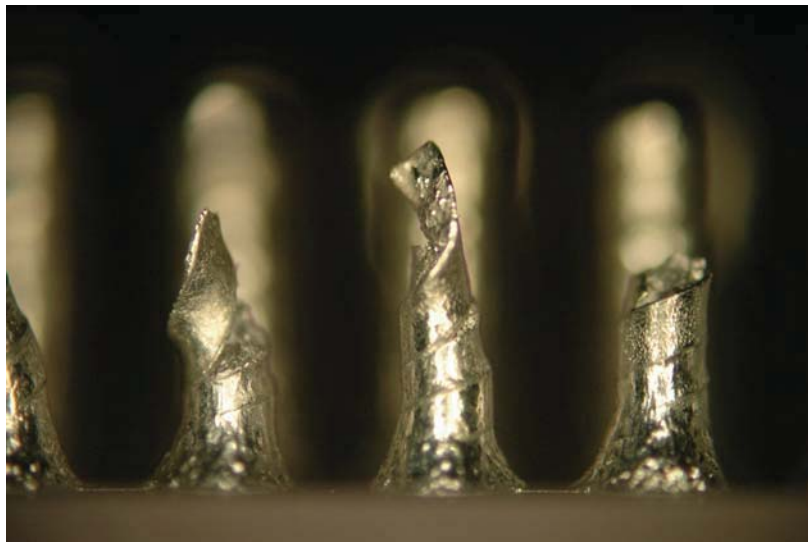


Figure 3. An image of a typical column failure mode found in Specimen #400.

Shown in Figure 4 is the plot of the averages of the pull forces as a function of aging time, for Specimen #400. Initially, there was a decrease in the average pull force after aging for 100 hrs. The average pull force was the same after that. Using student t-test calculations (assuming equal means), at a confidence level of 95%, it was found that there is a statistical difference between no aging and 100 hrs of aging. No statistical difference was found between 100 hrs and 247 hrs of aging. A statistical difference was found between 247 hrs and 500 hrs of aging. The student t-test calculations are shown in Appendix B. There was an overall decrease of 19% in the mean pull force over the aging time.

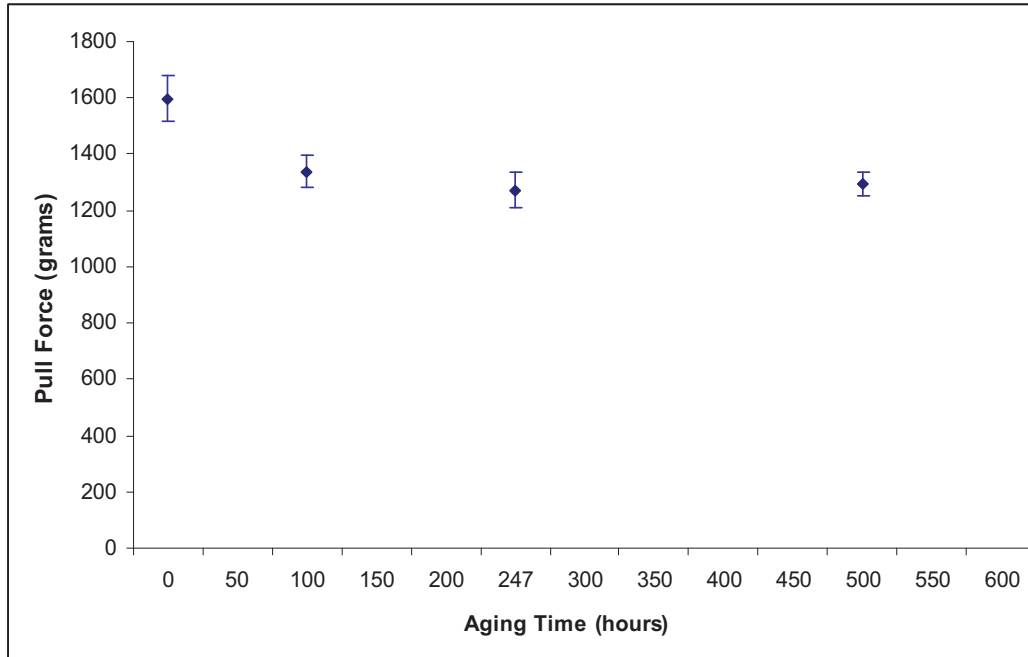


Figure 4. Pull force as a function of aging time, for Specimen #400.

Reference

1. Minitab Website (2007). *Paired t-Test* [Online]. Available at www.minitab.com (Accessed 2 June 2007).

Appendix A

Pull Test Results

Table A1. Pull test results for Specimen #300 after column attach.

Measurement #	Peak Force (g)	Failure Mode
1 (periphery)	1652	Column Failure
2 (periphery)	1652	Column Failure
3 (periphery)	1483	Column Failure
4 (periphery)	1624	Column Failure
5 (periphery)	1445	Column Failure
6 (periphery)	1522	Column Failure
7 (periphery)	1645	Column Failure
8 (periphery)	1662	Column Failure
9 (periphery)	1539	Column Failure
10 (periphery)	1630	Column Failure
11 (center)	1540	Column Failure
12 (center)	1517	Column Failure
13 (center)	1644	Column Failure
14 (center)	1607	Column Failure
15 (center)	1608	Column Failure

Table A2. Pull test results for Specimen #300 after aging for 100 hours.

Measurement #	Peak Force (g)	Failure Mode
1 (periphery)	1409	Column Failure
2 (periphery)	1477	Column Failure
3 (periphery)	1464	Column Failure
4 (periphery)	1465	Column Failure
5 (periphery)	1395	Column Failure
6 (periphery)	1365	Column Failure
7 (periphery)	1367	Column Failure
8 (periphery)	1315	Column Failure
9 (periphery)	1296	Column Failure
10 (periphery)	1309	Column Failure
11 (center)	1402	Column Failure
12 (center)	1392	Column Failure
13 (center)	1341	Column Failure
14 (center)	1351	Column Failure
15 (center)	1398	Column Failure

Table A3. Pull test results for Specimen #300 after aging for 247 hours.

Measurement #	Peak Force (g)	Failure Mode
1 (periphery)	1208	Column Failure
2 (periphery)	1295	Column Failure
3 (periphery)	1318	Column Failure
4 (periphery)	1297	Column Failure
5 (periphery)	1356	Column Failure
6 (periphery)	1280	Column Failure
7 (periphery)	1251	Column Failure
8 (periphery)	1341	Column Failure
9 (periphery)	1385	Column Failure
10 (periphery)	1243	Column Failure
11 (center)	1259	Column Failure
12 (center)	1417	Column Failure
13 (center)	1402	Column Failure
14 (center)	1324	Column Failure
15 (center)	1368	Column Failure

Table A4. Pull test results for Specimen #300 after aging for 500 hours.

Measurement #	Peak Force (g)	Failure Mode
1 (periphery)	1228	Column Failure
2 (periphery)	1249	Column Failure
3 (periphery)	1319	Column Failure
4 (periphery)	1246	Column Failure
5 (periphery)	1243	Column Failure
6 (periphery)	1257	Column Failure
7 (periphery)	1263	Column Failure
8 (periphery)	1270	Column Failure
9 (periphery)	1348	Column Failure
10 (periphery)	1303	Column Failure
11 (center)	1312	Column Failure
12 (center)	1351	Column Failure
13 (center)	1200	Column Failure
14 (center)	1281	Column Failure
15 (center)	1185	Column Failure

Table A5. Pull test results for Specimen #400 after column attach.

Measurement #	Peak Force (g)	Failure Mode
1 (periphery)	1592	Column Failure
2 (periphery)	1611	Column Failure
3 (periphery)	1648	Column Failure
4 (periphery)	1592	Column Failure
5 (periphery)	1511	Column Failure
6 (periphery)	1402	Column Failure
7 (periphery)	1451	Column Failure
8 (periphery)	1662	Column Failure
9 (periphery)	1653	Column Failure
10 (periphery)	1645	Column Failure
11 (center)	1666	Column Failure
12 (center)	1626	Column Failure
13 (center)	1644	Column Failure
14 (center)	1640	Column Failure
15 (center)	1628	Column Failure

Table A6. Pull test results for Specimen #400 after aging for 100 hours.

Measurement #	Peak Force (g)	Failure Mode
1 (periphery)	1271	Column Failure
2 (periphery)	1452	Column Failure
3 (periphery)	1269	Column Failure
4 (periphery)	1354	Column Failure
5 (periphery)	1270	Column Failure
6 (periphery)	1440	Column Failure
7 (periphery)	1315	Column Failure
8 (periphery)	1374	Column Failure
9 (periphery)	1353	Column Failure
10 (periphery)	1350	Column Failure
11 (center)	1319	Column Failure
12 (center)	1270	Column Failure
13 (center)	1361	Column Failure
14 (center)	1322	Column Failure
15 (center)	1354	Column Failure

Table A7. Pull test results for Specimen #400 after aging for 247 hours.

Measurement #	Peak Force (g)	Failure Mode
1 (periphery)	1240	Column Failure
2 (periphery)	1209	Column Failure
3 (periphery)	1210	Column Failure
4 (periphery)	1260	Column Failure
5 (periphery)	1417	Column Failure
6 (periphery)	1231	Column Failure
7 (periphery)	1216	Column Failure
8 (periphery)	1337	Column Failure
9 (periphery)	1210	Column Failure
10 (periphery)	1292	Column Failure
11 (center)	1380	Column Failure
12 (center)	1292	Column Failure
13 (center)	1248	Column Failure
14 (center)	1304	Column Failure
15 (center)	1247	Column Failure

Table A8. Pull test results for Specimen #400 after aging for 500 hours.

Measurement #	Peak Force (g)	Failure Mode
1 (periphery)	1397	Column Failure
2 (periphery)	1251	Column Failure
3 (periphery)	1305	Column Failure
4 (periphery)	1329	Column Failure
5 (periphery)	1334	Column Failure
6 (periphery)	1300	Column Failure
7 (periphery)	1285	Column Failure
8 (periphery)	1221	Column Failure
9 (periphery)	1261	Column Failure
10 (periphery)	1289	Column Failure
11 (center)	1303	Column Failure
12 (center)	1277	Column Failure
13 (center)	1297	Column Failure
14 (center)	1298	Column Failure
15 (center)	1267	Column Failure

Appendix B

Student t-test Calculations

Paired Student t-Test

A paired student t-test is used to test the mean difference between paired observations (such as before and after measurements) when the paired differences follow a normal distribution [1]. This test matches responses that are dependent or related in a pairwise manner, which allows the investigator to account for variability between the pairs. This usually results in a smaller error, thus increasing the sensitivity of the hypothesis test or confidence interval.

To determine statistical significance, the p-test value is calculated. The p-value determines if it is appropriate to reject the null hypothesis and accept the alternative hypothesis instead [1]. It has values in the range of 0 to 1. When performing this test, an α -value is usually chosen. If the p-value of the test-statistic is less than the α -value, then the null hypothesis is rejected, and the alternative hypothesis is accepted. If the p-value is greater than the α -value, the null hypothesis is accepted. The α -value at 95% confidence level is 0.05. The hypotheses used in this study are:

- Null Hypothesis: The mean pull forces are the same.
- Alternative Hypothesis: The mean pull forces are different.

Student t-test Results for Specimen #300

Table B1. Paired t-test between no aging and 100 hrs of aging.

	N	Mean	StDev
No aging	15	1585	70
100-hr Aging	15	1383	56
T-Test of mean difference = 0 (vs not = 0): T-Value = 2.14, P-Value = 1.11×10^{-6}			

Table B2. Paired t-test between 100 hrs of aging and 247 hrs of aging.

	N	Mean	StDev
100-hr Aging	15	1383	56
247-hr Aging	15	1316	62
T-Test of mean difference = 0 (vs not = 0): T-Value = 2.14, P-Value = 0.01			

Table B3. Paired t-test between 247 hrs of aging and 500 hrs of aging.

	N	Mean	StDev
100-hr Aging	15	1316	62
247-hr Aging	15	1270	49
T-Test of mean difference = 0 (vs not = 0): T-Value = 2.14, P-Value = 0.03			

Student t-test Results for Specimen #400

Table B4. Paired t-test between no aging and 100 hrs of aging.

	N	Mean	StDev
No aging	15	1598	80
100-hr Aging	15	1338	57
T-Test of mean difference = 0 (vs not = 0): T-Value = 2.14, P-Value = 1.79×10^{-7}			

Table B5. Paired t-test between 100 hrs of aging and 247 hrs of aging.

	N	Mean	StDev
100-hr Aging	15	1338	57
247-hr Aging	15	1273	64
T-Test of mean difference = 0 (vs not = 0): T-Value = 2.14, P-Value = 0.02			

Table B6. Paired t-test between 247 hrs of aging and 500 hrs of aging.

	N	Mean	StDev
100-hr Aging	15	1273	64
247-hr Aging	15	1294	41
T-Test of mean difference = 0 (vs not = 0): T-Value = 2.14, P-Value = 0.2			

Appendix C

XRF Data

Table C1. Composition and thickness of incoming finish for Specimen # 300.

Meas. #	Sn-Pb (μm)	Sn (wt%)	Date	Time
1	35.64	63.23	1/29/08	3:22:02 PM
2	30.21	65.11	1/29/08	3:25:42 PM
3	26.93	71.49	1/29/08	3:26:22 PM
4	33.23	66.06	1/29/08	3:27:03 PM
5	30.62	62.33	1/29/08	3:27:46 PM
6	32.71	61.83	1/29/08	3:28:25 PM
7	44.23	60.16	1/29/08	3:29:07 PM
8	32.51	59.86	1/29/08	3:29:48 PM
9	31.20	56.29	1/29/08	3:30:29 PM
10	38.55	64.57	1/29/08	3:31:10 PM

Table C2. Composition and thickness of incoming finish for Specimen # 400.

Meas. #	Sn-Pb (μm)	Pb (wt%)	Date	Time
1	40.54	45.29	1/29/08	3:37:46 PM
2	35.21	48.14	1/29/08	3:38:27 PM
3	35.88	46.88	1/29/08	3:39:10 PM
4	28.35	53.62	1/29/08	3:39:52 PM
5	26.15	52.38	1/29/08	3:40:36 PM
6	24.87	52.80	1/29/08	3:41:18 PM
7	34.82	54.93	1/29/08	3:42:00 PM
8	43.02	46.57	1/29/08	3:42:39 PM
9	39.61	45.46	1/29/08	3:43:20 PM
10	33.84	46.58	1/29/08	3:44:00 PM

Table C3. Composition and thickness of finish for Specimen # 300 after column attach.

Meas. #	Sn (wt%)	Pb (wt%)	Date	Time
1	30.53	69.47	1/31/08	6:22:36 PM
2	29.81	70.19	1/31/08	6:23:21 PM
3	29.66	70.34	1/31/08	6:24:08 PM
4	31.76	68.24	1/31/08	6:24:53 PM
5	29.17	70.83	1/31/08	6:25:39 PM
6	30.35	69.65	1/31/08	6:26:25 PM
7	28.92	71.08	1/31/08	6:27:10 PM
8	34.37	65.63	1/31/08	6:27:55 PM
9	30.20	69.80	1/31/08	6:28:40 PM
10	33.39	66.61	1/31/08	6:29:26 PM

Table C4. Composition and thickness of finish for Specimen # 400 after column attach.

Meas. #	Sn (wt%)	Pb (wt%)	Date	Time
1	32.55	67.45	1/31/08	6:30:12 PM
2	31.71	68.29	1/31/08	6:30:57 PM
3	29.35	70.65	1/31/08	6:31:44 PM
4	31.55	68.45	1/31/08	6:32:29 PM
5	32.41	67.59	1/31/08	6:33:15 PM
6	31.67	68.33	1/31/08	6:34:00 PM
7	35.89	64.11	1/31/08	6:34:45 PM
8	28.35	71.65	1/31/08	6:35:32 PM
9	30.65	69.35	1/31/08	6:36:17 PM
10	35.12	64.88	1/31/08	6:37:02 PM

Appendix D

Images of Column Grid Arrays After Removal of Interposer

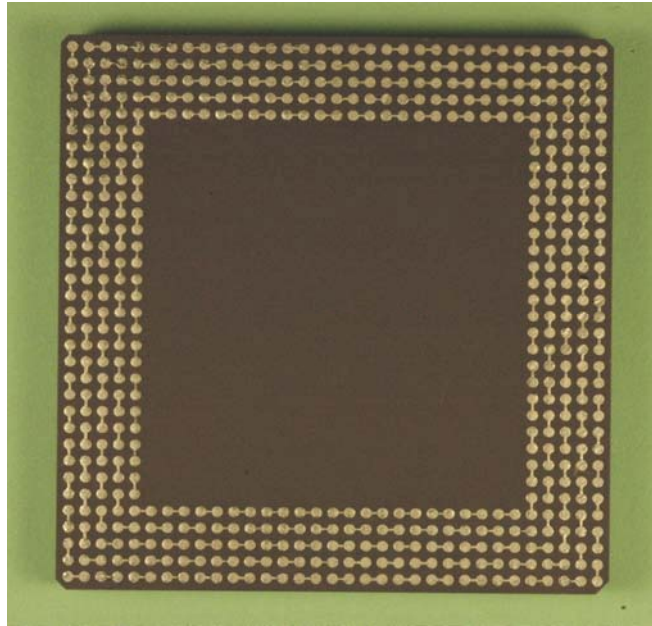


Figure D1. Image of Specimen #300 after interposer removal.

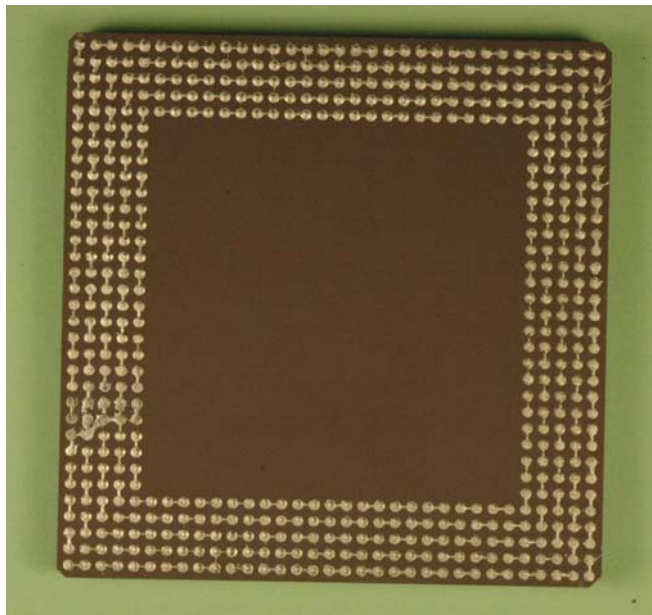


Figure D2. Image of Specimen #400 after interposer removal.